Matrix Metalloproteinase 9 and Osteopontin Interact to Support Synaptogenesis in the Olfactory Bulb after Mild Traumatic Brain Injury

Melissa A. Powell, Raiford T. Black, Terry L. Smith, Thomas M. Reeves, and Linda L. Phillips

Abstract

Olfactory receptor axons reinnervate the olfactory bulb (OB) after chemical or transection lesion. Diffuse brain injury damages the same axons, but the time course and regulators of OB reinnervation are unknown. Gelatinases (matrix metalloproteinase [MMP]2, MMP9) and their substrate osteopontin (OPN) are candidate mediators of synaptogenesis after central nervous system (CNS) insult, including olfactory axon damage. Here, we examined the time course of MMP9, OPN, and OPN receptor CD44 response to diffuse OB injury. FVBV/NJ mice received mild midline fluid percussion insult (mFPI), after which MMP9 activity and both OPN and CD44 protein expression were measured. Diffuse mFPI induced time-dependent increase in OB MMP9 activity and elevated the cell signaling 48-kD OPN fragment. This response was bimodal at 1 and 7 days post-injury. MMP9 activity was also correlated with 7-day reduction in a second 32-kD OPN peptide. CD44 increase peaked at 3 days, delayed relative to MMP9/OPN response. MMP9 and OPN immunohistochemistry suggested that deafferented tufted and mitral neurons were the principal sites for these molecular interactions. Analysis of injured MMP9 knockout (KO) mice showed that 48-kD OPN production was dependent on OB MMP9 activity, but with no KO effect on CD44 induction. Olfactory marker protein (OMP), used to identify injured olfactory axons, revealed persistent axon damage in the absence of MMP9. MMP9 KO ultrastructure at 21 days post-injury indicated that persistent OMP reduction was paired with delayed removal of degenerated axons. These results provide evidence that diffuse, concussive brain trauma induces a post-injury interaction between MMP9, OPN, and CD44, which mediates synaptic plasticity and reinnervation within the OB.

Keywords: metalloproteinase; olfactory bulb; osteopontin; synaptogenesis

Introduction

REACTIVE SYNAPTOGENESIS is well described after targeted deafferentation, characterized by phases of axon damage, glial removal of cellular debris, sprouting of new terminals, and stabilization of nascent synapses. Whereas these stages are best detailed in the hippocampus,[1] transection of the olfactory nerve[2] can similarly induce synaptogenesis within the olfactory bulb (OB). Diffuse axonal insult associated with traumatic brain injury (TBI) can also promote reactive synaptogenesis, but the extent of OB axon damage and synaptic reorganization is not well understood. Recently, we reported that mild fluid percussion injury (mFPI) is sufficient to generate OB axonal damage and subsequent synaptic plasticity.[3] Under conditions of diffuse mFPI, we observed significant proteolysis of OB αII-spectrin, as well as a reduction of olfactory marker protein (OMP), each supporting pre-synaptic olfactory neuron (ORN) axon degeneration. Time-dependent induction of OB glial reactivity and growth-associated protein 43 growth factor elevation also confirmed onset of post-injury reinnervation processes. Interestingly, such injury-induced plasticity can be mediated by molecules expressed in the extracellular matrix (ECM) around affected synapses.[4–6] For example, extracellular proteoglycans—osteopontin (OPN) and matrix metalloproteinases (MMPs)—can influence the outcome of this plasticity in both adaptive and maladaptive forms.[7–16] Among the MMPs, gelatinases exhibit elevated expression and activity correlated with time-dependent deafferentation and synaptic repair, suggesting that they may be especially important for successful synaptogenesis.

Gelatinases A and B (MMPs 2 and 9) have been studied extensively during functional recovery after brain injury.[5,7,17–20] However, few studies have probed the role of MMPs 2 and 9 after OB insult, the majority utilizing models of more-severe targeted deafferentation. After focal ORN lesion and olfactory nerve axotomy, expression of the two gelatinases increases.[21–23] MMP9 protein peaks significantly at 5 days post-injury, implicating a prominent role in the acute degenerative process, whereas MMP2

upregulation is delayed and less robust, suggesting that MMP2 contributes more to synaptic reinnervation. These differences highlight the importance of the time course of MMP response during OB synaptic repair. MMP9 elevation has consistently been linked with brain hemorrhage and spinal cord injury,[24–26] as well as in animal models of axotomy,[9,22] yet exact gelatinase-mediated mechanisms contributing to OB synaptic recovery are unknown. We propose that diffuse mFPI can be used to define the time course of post-injury MMP9 activity and identify MMP9 substrates critical to OB synaptic repair after brain injury.

One novel MMP substrate associated with synaptic repair is the cytokine, OPN. OPN is a phosphoprotein correlated with neuro-protective function in models of brain injury.[9,27–30] It is lysed by MMP9,[31–33] which typically occurs upon its secretion into the ECM. Upon cleavage, integrin receptor-binding RGD and SVVYGLR sequences within OPN are exposed on the larger, N-terminal fragment.[34] This exposure permits cell signaling that facilitates adhesion, migration, and proliferation through $\alpha_v\beta_3$ vitronectin receptors, as well as the hyaluronic acid receptor, CD44, a signaling peptide important for directing migration and paracrine response between reactive glial cells.[34–36] MMP9 also produces a smaller, C-terminal OPN fragment, which can either interact with CD44 receptors or go on to further lysis and recycling. Interestingly, CD44 expression increases in tandem with OPN after cortical cryolesion,[37] transient forebrain ischemia,[38] and penetrating focal brain injury.[39] Because such increases in OPN and CD44 are reported within reactive glia, we hypothesized that OB gliosis after mFPI may be dependent upon MMP9-generated OPN signaling, acting through targeted CD44 cell-surface receptors.

Manipulation of MMP9 would be one approach to test whether production of OPN fragments and increased CD44 cell signaling influences OB synaptic recovery after mFPI. Typically, post-injury MMP function is blocked by either applying pharmacological inhibitors[8,15,19,40–43] or using MMP KO (knockout) animals.[17,19,23,43–50] In previous studies we showed that OPN processing into signaling fragments during reactive synaptogenesis is reduced with pharmacological inhibition of MMP activity.[5,9] Because MMP family members are highly homologous, and sites of enzyme inhibition can be non-selective for MMP type, MMP9 KO mice permit a more specific method to test the enzyme's role in OB plasticity. In some brain injury models, MMP9 KO was reported to attenuate both structural[45] and functional[51] measures of synaptic recovery. From these data, we posited that MMP9 KO mice subjected to mFPI would reveal a time-dependent interaction between MMP9 and OPN within the injured OB. We also predicted that MMP9 loss would alter the time course of ORN axon degeneration and attenuate CD44 expression as a correlate of altered glial reactivity.

In the present study, we first documented the post-injury time course of gelatinase activity, OPN fragment formation, and CD44 receptor expression within the OB of FVB/NJ mice subjected to mFPI. Post-injury survival intervals were selected to represent periods of acute/subacute degeneration (1, 3, and 7 days) and early ORN axon regeneration (21 days), as previously described.[3,52–54] These data were correlated with immunohistochemical (IHC) probe of MMP9 and OPN tissue distribution in the deafferented glomerular layer (GL). Here, we provide evidence for a time-dependent post-injury interaction between MMP9 and OPN, which has temporal correlates with both OB glial reactivity and expression of CD44 cell-surface receptors.

Potential MMP9/OPN interaction was further tested using MMP9 KO mice (on FVB/NJ background) to determine whether MMP9 loss altered mFPI induced OPN proteolysis and CD44 upregulation. We also used OMP to map ORN axon integrity and compared post-injury differences in GL synaptic profile between wild-type (WT) and MMP9 KO at 21 days after mFPI. IHC was conducted to confirm any post-injury differences in glial reactivity attributed to MMP9 loss. Comparison of WT and MMP9 KO results support the hypothesis that post-injury MMP9 activity generates OPN signaling fragments in the OB, as well as influences the onset and progression of ORN axon degeneration mapped by change in OMP expression. In addition, transmission electron microscopy (TEM) data revealed that loss of MMP9 and reduced OPN signaling shifted the time course of degenerative debris removal during reactive synaptogenesis, resulting in attenuated synaptic reorganization during onset of reinnervation. Together, the present results demonstrate that induced MMP9 activity supports OB synaptic plasticity after mFPI, an effect mediated, in part, through processing of OPN signaling peptides. These OPN signals likely operate through affected post-synaptic neurons and involve CD44 receptors.

Methods

Experimental animals

All procedures met national guidelines for care and use of laboratory animals, and all experimental protocols were approved by the Virginia Commonwealth University (VCU) Institutional Animal Care and Use Committee. FVB/NJ WT and MMP9 KO adult male mice (The Jackson Laboratory, Bar Harbor, ME) were housed (4 littermates/cage) under a temperature- (22°C) and humidity-controlled environment, with food and water *ad libitum*, and subjected to a 12-h dark-light cycle. Mice of each strain (20–30 g; 8–11 weeks old) were randomly selected and subjected to midline mFPI or sham injury. In preliminary experiments, FVB/NJ WT and MMP9 KO mice subjected to sham-injury ($n=4$/group) failed to show differences in OMP, a principal molecular measure of ORN axon injury used in the study. From these data, FVB/NJ WT sham-injured cases were selected, *a priori*, to serve as injury controls. Subsets of injured and WT sham-injured groups (FVB/NJ WT Sham [$n=4$], FVB/NJ WT mFPI [$n=53$], and MMP9 KO mFPI [$n=36$]) were allowed to survive for either 1, 3, 7, or 21 days before molecular, histological, or ultrastructural analyses.

Surgery preparation and injury

Mice were anesthetized with isoflurane (4% in 100% O_2 carrier gas) and maintained on 2.5% isoflurane in carrier gas delivered through a nose cone. Once stabilized in a stereotaxic frame, heads were shaved, body temperature maintained at 37°C by Gaymar T/Pump water pump (Gaymar Industries Inc, Orchard Park, NY), and heart rate (bpm), arterial oxygen saturation (percent O_2), breath rate (brpm), and pulse/breath distension (μm) monitored by pulse oximetry (MouseOx; Starr Life Sciences, Oakmont, PA). Mice then received a dorsal cranial incision and a 2.7-mm craniectomy prepared over the midline, centered between bregma and lambda. Without damaging the underlying dura, a Leur-Loc syringe hub was cemented to the skull surrounding the craniectomy and dental acrylic poured around the hub to stabilize the site. Topical anesthetic/antibiotic was applied to the incision site and mice housed in recovery cages. After 1 h of surgical recovery, mice were anesthetized for 4 min (4% isoflurane, 100% O_2) and subjected to mFPI as previously described.[55,56] The device consisted of a 60×4.5 cm Plexiglas water-filled cylinder, fitted at one end with a piston mounted on O-rings, with the opposite end housing a pressure transducer (EPN-0300A; Entran Devices, Inc.,

Fairfield, NJ). At the time of injury, the Leur-Loc fitting, filled with saline, was attached to the transducer housing. Injury was produced by a metal pendulum striking the piston, transiently injecting a small volume of saline into the cranial cavity, and briefly deforming the brain tissue (20-ms pulse duration). The resulting pressure pulse was recorded extracranially and registered 1.3 ± 0.1 atm of pressure. After injury, all mice were promptly ventilated with room air until spontaneous breathing resumed. The duration of suppression of the righting reflex $(5.0 \pm 2.0 \text{ min})$ was used as an index of traumatic unconsciousness. Once righting reflex was determined, mice were reanesthetized for hub removal, scalp suture, and topical anesthetic/antibiotic application. FVB/NJ WT sham-injured controls received the same surgical preparation, anesthesia, and connection to the injury device, except that the intracranial pressure pulse was not applied. All animals were returned to their home cages and assessed for weight loss, locomotion, and eye/nose exudate once per day until weights stabilized.

Protein extraction

FVB/NJ WT and MMP9 KO mice were anesthetized with 4% isoflurane in carrier gas of 100% O_2 for 4 min, then sacrificed by decapitation at 1, 3, 7, or 21 days after FPI or sham injury, with bilateral OBs dissected (n = 4–7/group) for assessment of protein expression. Tissue samples were homogenized on ice in $100 \mu L$ of radioimmunoprecipitation assay lysis buffer (EMD Millipore, Billerica, MA) and centrifuged at $14,000g$ for 20 min at 4°C. Supernatant was aliquoted and stored at −80°C. Before blot or zymography analysis, protein concentration was determined using Pierce BCA Protein Assay Reagent (Thermo-Fisher, Waltham, MA) and the FLUOstar Optima plate reader (BMG Labtech, Inc., Cary, NC).

Western blot analysis

Western blot (WB) probe was carried out utilizing Bio-Rad products (Bio-Rad Laboratories, Hercules, CA). Twenty micrograms of protein was prepared in WB XT Sample Buffer and reducing agent (Bio-Rad Laboratories), then denatured at 95°C for 5 min (except for unreduced CD44 WB protocol, where samples were prepared without reducing agent). Samples were electrophoresed on 4–12% or 12% Bis-Tris Criterion XT gels (200 v × 45 min in 3-morpholinopropane-1-sulfonic acid running buffer), then protein transferred onto polyvinylidene fluoride membranes (1 h at 100 V). Post-blotted gels were stained with 0.1% Coomassie brilliant blue (Sigma-Aldrich, St. Louis, MO) in 40% MeOH +10% glacial acetic acid, then destained at room temperature (RT) to confirm protein load and even transfer. Membranes were rinsed with deionized water and Tris-buffered saline (TBS) before blocking with 5% milk TBS-Tween (mTBS-T). Blots were then incubated in 5% mTBS-T overnight (4°C) with individual primary antibodies to either OPN (1:500; R&D Systems, Minneapolis, MN; and 1:500; Rockland Immunochemicals Inc., Limerick, PA), CD44 (1:500; BD Biosciences, San Jose, CA), or OMP (1:20,000, Wako, Richmond, VA). After primary incubation, membranes were washed with mTBS-T, then incubated with appropriate horseradish peroxidase (HRP)-linked secondary antibodies (immunoglobulin G [IgG] bovine antigoat, IgG bovine antirabbit [1:15,000; Santa Cruz Biotechnology, Dallas, TX], IgG goat antimouse, and IgG goat antirat [1:15,000; Rockland Immunochemicals] in mTBS-T for 1 h at RT. Finally, blots were washed with mTBS-T and antibody binding visualized using Super Signal Dura West chemiluminescence substrate (Thermo-Fisher). WB images were captured with Syngene G:Box and positive band signal subjected to densitometric analysis (relative optical density; ROD) with Gene Tools software (Syngene, Frederick, MD). Protein data were ex-

pressed as percent change relative to paired FVB/NJ WT sham-injured cases run on the same transferred gel. Cyclophillin A (EMD Millipore) or beta actin (Sigma-Aldrich) was used as load controls for signal detection.

Immunohistochemistry

At 3, 7, and 21 days post-injury, FVB/NJ WT injured and sham mice, along with MMP9 KO mice (n = 4/group) were prepared for fluorescent IHC analysis according to a published protocol.[15] Animals were anesthetized with sodium pentobarbital (400 mg/kg, intraperitoneally [i.p.]) and transcardially perfused with 0.9% saline followed by 4% paraformaldehyde (PFA) in phosphate buffer (0.1 M of $NaHPO_4$, pH = 7.4), after which brains with attached OBs were extracted and placed in fixative for 24 h before transfer to 0.03% NaN_3 in 1.0 M of phosphate-buffered saline (PBS). For IHC, fixed brains were cryoprotected in 30% sucrose for 3 days, then sucrose solutions exchanged each day. Frontal lobes were blocked and attached bulbs mounted in Tissue Tek media (Thermo-Fisher) and stored at −80°C. Coronal cryostat OB sections ($13 \mu M$) were collected using a Cryostar™NX70; Cryotome™FSE; HM525 NX cryostat (Thermo-Fisher, Waltham, MA) and prepared for immunofluorescence visualization.

Free-floating sections were first permeabilized in 5% peroxidase for 30 min. After a wash with PBS, tissues were pre-incubated in blocking buffer (fish gelatin in PBS +0.05% Triton X-100) to prevent non-specific binding and then incubated overnight in primary antibody (OPN, 1:40; R&D Systems; MMP9, 1:100; R&D Systems; microtubule-associated protein 2 [MAP2], 1:500; EMD Millipore; tyrosine hydroxylase [TH], 1:300; EMD Millipore; glial fibrillary acidic protein [GFAP], 1:20,000; Dako, Glostrop, Denmark; ionized calcium-binding adaptor protein 1 [IBA1] for microglia, 1:300; Wako, Richmond, VA; and cholecystokinin [CCK], 1:20; R&D Systems) at 4°C. Sections were next washed with PBS, placed in blocking buffer for 30 min, after which they were incubated with secondary fluorescent antibody (Alexa-Fluor 488 donkey antigoat, 1:1000 and Alexa-Fluor 594 donkey antirabbit, 1:1000; Thermo-Fisher) in Blotto for 1 h at RT. Slices were then PBS washed, equilibrated in phosphate buffer, and mounted on Superfrost Plus slides (Fisher Scientific, Pittsburgh, PA) with Vectashield +4′,6-diamidino-2-phenylindole (Vector Laboratories, Burlingame, CA). IHC signal was visualized on the Zeiss LSM 700 (Carl Zeiss, Thornwood, NY) confocal microscope (VCU Microscopy Core).

Gelatin zymography

Zymographic enzyme assay was performed using previously described methods.[9,57] Briefly, 20 μg of protein from the same OB extracts used for WB were prepared with 2 × Tris-glycine sodium dodecyl sulfate sample buffer, then separated by gelatin electrophoresis (at 4°C, 45 V for 1.5 h) on Novex® 10% Zymogram gels (Thermo-Fisher). Gels were renatured in Novex Zymogram Renaturing Buffer (Thermo-Fisher) for 30 min at room temperature before development in Novex Zymogram Developing Buffer over 6 days at 37°C. Gelatin lysis was visualized with Coomassie brilliant blue (Sigma-Aldrich). Zymogram signal was captured on a Syngene G:BOX and densitometry analyzed as ROD with Gene Tools software (Syngene). Enzyme activity was expressed as percent change relative to paired FVB/NJ WT sham-injured controls run on the same gel.

Transmission electron microcopy

At 21 days after FPI, FVB/NJ WT injured, MMP9 KO injured, and FVB/NJ WT sham-injured mice (n = 3/group) were anesthetized
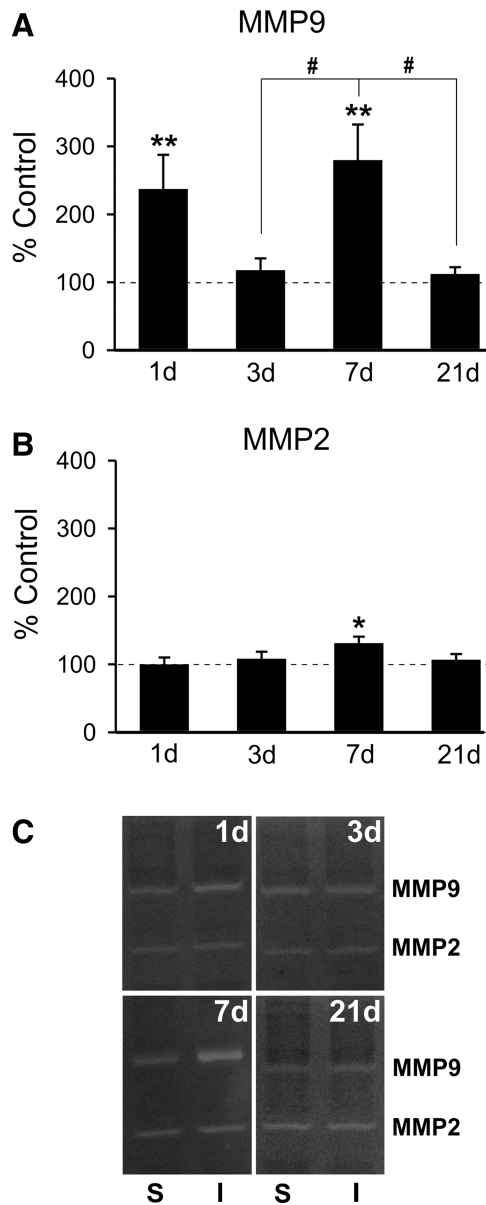
FIG. 1. mFPI increases OB gelatinase activity. (**A**) Post-injury OB zymography revealed biphasic elevation of MMP9 activity relative to sham controls. Acute increase of enzyme activity occurred at 1 day after injury, normalized at 3 days, and re-emerged in a second peak of MMP9 activation at 7 days. By 21 days, activity had again returned to control values. Pos- hoc analysis showed 7-day proteolysis different from that at both 3 and 21 days. (**B**) Modest increase in MMP2 activity over sham controls was limited to 7 days post-injury. MMP2 activity was not different from controls at 1, 3, or 21 days post-injury. (**C**) Representative zymogram images of sham (left lane in pair), injured (right lane in pair). WB results are expressed as percent of sham control ROD (100% dashed line). S=sham; I=injured; *$p<0.05$ versus sham; #$p<0.05$; $n=4$–7/group. mFPI, mild fluid percussion injury; OB, olfactory bulb; MMP, matrix metalloproteinase; ROD, relative optical density; WB, western blot.

with sodium pentobarbital (400 mg/kg, i.p.), transcardially perfused with mixed aldehyde fixative (2% PFA and 2.5% glutaraldehyde) in 0.1 M of phosphate buffer (pH, 7.2). Brains were removed and post-fixed overnight at 4°C before processing for TEM as described previously.[56] OBs were next blocked in the

sagittal plane, placed in 1% osmium tetroxide (0.1 M of cacodylate buffer), and processed for embedding with Epon resin (Embed; Electron Microscopy Sciences, Hatfield, PA). After curing, OB areas containing glomeruli were mounted, and both semithin (0.5 μm) and ultrathin (silver, 600 Å) sections were cut with a Leica EM UC6i ultramicrotome (Leica Microsystems, Wetzlar, Germany). Semithin sections were used to guide subsequent ultrastructural sampling. Ultrathin sections were collected on Formvar-coated slotted grids and observed on a JEOL JEM-1230 electron microscope (JEOL USA, Inc., Peabody, MA), equipped with a Gatan Ultra Scan 4000SP CCD camera (Gatan, Inc., Pleasanton, CA).

Statistical analysis

Changes in protein level and enzyme activity induced by injury were evaluated using the generalized linear model and multi-variate analysis of variance routines in SPSS software (v.22; International Business Machines, Corp., Armonk, NY). Normality (Kolmogorov-Smirnov Test) and homogeneity of variance (Levene Statistic) were confirmed before analysis of variance analyses. The Duncan multiple-range test was used for post-hoc pair-wise group comparisons. Results are reported as mean ± standard error of the mean. An alpha level of 0.05 was used in all analyses.

Results

Olfactory bulb matrix metalloproteinase 9 activity and protein distribution after mild fluid percussion injury

Previous brain injury studies show that secreted MMPs and inflammatory cytokines contribute to both acute pathophysiology and chronic repair mechanisms.[5,58,59] Increases in gelatinases MMP 2 and 9 were reported during OB pre-synaptic degeneration induced by either ORN knife-cut axotomy or chemical lesion[21–23]; however, OB MMP response to mFPI has not been determined. Here, we first assessed OB protein extracts with zymography to determine whether diffuse mFPI would alter gelatinase activity 1–21 days post-injury. Overall, we found time-dependent increase in MMP9 activity, with a small, but significant, rise in MMP2 proteolysis limited to one survival interval (Fig. 1A,B). At 1 day post-injury, FVB/NJ WT mice exhibited a 2-fold rise in MMP9 activity versus sham controls (236.85±50.71; $p<0.01$). By contrast, 1-day MMP2 lysis was not different from control values (99.48±10.63), and activity for both gelatinases remained equivalent to that of sham injured at 3 days after mFPI (117.40±17.71; 107.69±10.89). Interestingly, at 7 days after injury, we also found a second elevation in MMP9 activity, nearly 3-fold over sham injured cases (279.54±52.58; $p<0.001$), accompanied by a small 31% rise in MMP2 activity (130.75±10.02; $p<0.05$). By 21 days, the period typically marking ORN axon reinnervation, gelatinase activity was not different from sham-injured levels (111.79±10.42; 106.43±8.66). Post-hoc analysis showed that the 7-day rise in MMP9 activity was also significantly increased relative to 3- and 21-day post-injury time points ($p<0.05$), suggesting critical periods of MMP activation at 1 and 7 days post-injury. This MMP2 and MMP9 post-injury activity indicates time-dependent roles for each enzyme during the recovery process. Specifically, MMP9 appears to play a critical role in both acute degeneration (1-day) and early re-innervation (7-day) phases of reactive synaptogenesis in the deafferented OB.
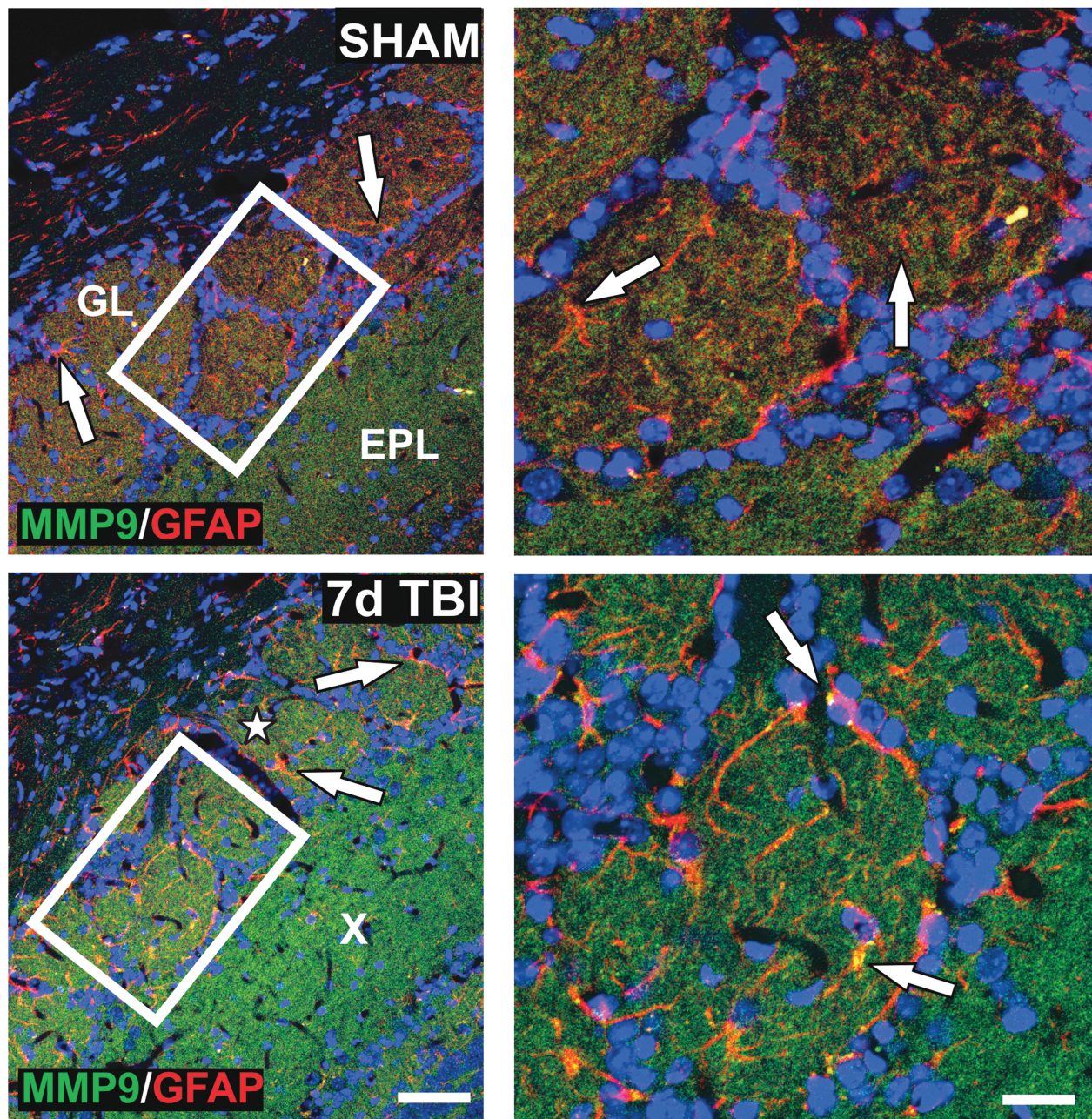
FIG. 2. mFPI increases OB gelatinase protein distribution. Imaging shows low, punctate signal for MMP9 (green) in GL and EPL in sham cases. Nonreactive, GFAP+ astrocytes (red) localized to the GL (white arrows). MMP9 was increased in the same layers 7 days after mFPI (white star = GL; X = EPL) and in reactive astrocytes (white arrows). High magnification of boxed areas at right show MMP9 expression within GL astrocytes (white arrows). These IHC results correlate with 7-day rise in MMP9 activity. Bar = 50 μm, left panels; bar = 20 μm, right panels; n = 3/group. EPL, external plexiform layer; GFAP, glial fibrillary acidic protein; GL, glomerular layer; IHC, immunohistochemical; mFPI, mild fluid percussion injury; MMP, matrix metalloproteinase; OB, olfactory bulb.

Because secreted MMP9 can facilitate intercellular signals for glial/neuronal reorganization after injury,[5] we next mapped OB MMP9 protein distribution at 7 days post-injury. Given that astrocytes can secrete MMPs and are the prominent glia of OB glomeruli, we performed IHC colocalization of MMP9 and GFAP after mFPI. GFAP+ astrocytes surrounding glomeruli did contain MMP9; however, MMP9 was also elevated within the axodendritic fields of the GL and external plexiform layer (EPL; Fig. 2). Together, these zymography and IHC results suggest a complex enzyme response to mFPI within the OB, where both neurons and astrocytes might generate and secrete MMP9 for local processing of matrix proteins to support reactive synaptogenesis.

Osteopontin fragment expression in olfactory bulb after mild fluid percussion injury

Studies in deafferented hippocampus show that OPN can influence synaptic plasticity, where its RGD integrin signaling fragment
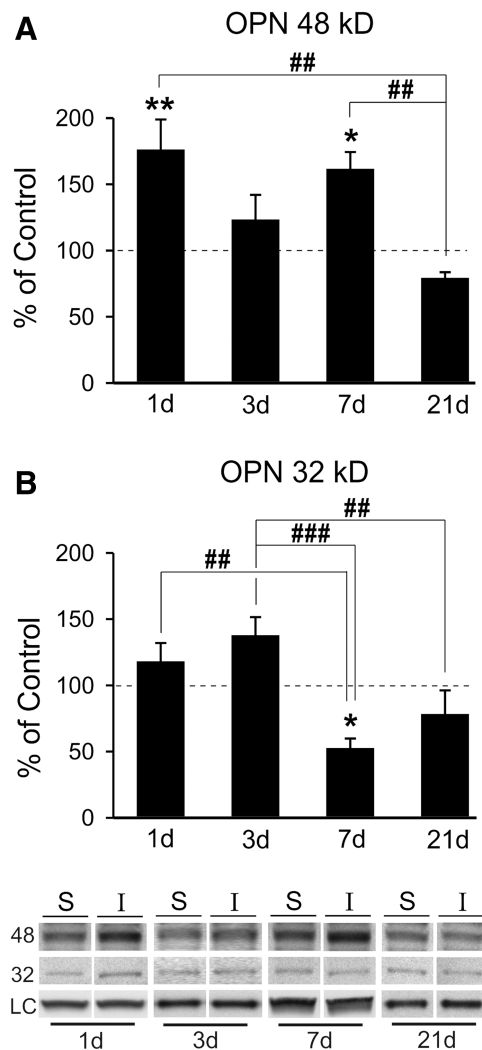
FIG. 3. mFPI induces generation of OPN signaling fragments in the OB. (**A**) Post-injury analysis of 48-kD OPN showed significant elevation of the RGD signaling fragment at 1 and 7 dayd relative to sham controls. At both 3 and 21 days post-injury 48-kD OPN levels were not different from controls. Post-hoc analysis confirmed that 1- and 7-day protein signal was significantly elevated compared with that of 21 days. This pattern of 48-kD OPN correlates with peak MMP9 activity. (**B**) Only one post-injury change in 32-kD OPN peptide was observed, a reduction from sham controls at 7 days. Post-hoc analysis showed the 7-day reduction was significantly lower than both 1- and 3-day signal, as well as a difference between 3- and 21-day signal. Results expressed as percent of sham control ROD (100% dashed line). Representative blot images, with cyclophilin A and β-actin load controls, illustrated below. *$p < 0.05$, **$p < 0.01$ versus sham control; #$p < 0.05$; ##$p < 0.01$; ###$p < 0.001$; $n = 4$–7/group. mFPI, mild fluid percussion injury; MMP, matrix metalloproteinase; OPN, osteopontin; ROD, relative optical density.

is associated with glial reactivity, degenerative terminal removal, and adaptive synaptic recovery.[9] Moreover, this RGD fragment can be generated by MMP proteolysis of OPN,[31,32,34] leading us to examine the time-dependent generation of OPN fragments in the OB after mFPI. OB protein extracts from FVB/NJ WT mice were probed for OPN expression over time post-injury, using an anti-

body that identifies these fragments. MMP lysis of OPN can occur at the RGD/SVVYGLR region, generating two signaling fragments: an amino terminal portion with accessible RGD sequence and a carboxy terminal peptide.[31,32,34] Our WB probe showed the generation of these two principal OPN forms at 48 and 32kD (Fig. 3). The 48-kD integrin signaling RGD fragment was significantly elevated over sham controls at 1 (76%) and 7 days (62%) after injury (176.06 ± 22.81, $p < 0.01$; 161.53 ± 12.76, $p < 0.05$), which was correlated with elevated MMP9 activity (Fig. 3A; see again, Fig. 1A). Interestingly, whereas variance of signal for this fragment was observed at 3 and 21 days post-injury, measures were not different from sham-injured cases (123.22 ± 18.77; 79.09 ± 4.49). Post-hoc analysis revealed that 48-kD OPN signal at 21days was significantly different from both 1- and 7-day elevations ($p < 0.01$). Concurrent rise in MMP9 activity and 48-kD OPN over 1–7 days after mFPI and their attenuation by 21 days support a dual OPN signaling during OB synaptic reorganization. By contrast, the 32-kD OPN carboxy terminal fragment, lacking the RGD integrin-binding sequence, exhibited a different post-injury pattern (Fig. 3B). Here, the only significant change from controls was a 53% reduction at 7 days (52.52 ± 7.26; $p < 0.05$). Whereas some variability in expression occurred for the 32-kD OPN at 1, 3, and 21 days after mFPI, none of these changes were significant (117.90 ± 14.02; 137.61 ± 13.85; and 78.11 ± 18.10). Again, post-hoc analysis confirmed time-dependent changes in this OPN fragment. More acute 1- and 3-day levels were different from the reduced 32-kD OPN expression at 7 days ($p < 0.01$, $p < 0.001$; Fig. 3B), and a 3-day trend toward elevation in this fragment was also different from 21-day measures ($p < 0.01$). Notable expression differences between the two OPN fragments were observed: 32-kD OPN failed to show any acute 1-day induction, and 32-kD OPN was significantly reduced at 7 days when 48-kD OPN was prominently elevated. This may be attributed to the fact that increased MMP activity drives a progressive proteolysis of the non-RGD carboxy-terminal sequence.[34] Such correlates highlight OPN's role in OB reactive synaptogenesis and point to a predominant role for the 48-kD fragment. In order to test whether this OPN fragment generation might affect OB cell signaling, we mapped post-injury cellular localization of OPN.

Post-injury osteopontin expression in neurons of deafferented olfactory bulb

We initially performed IHC to assess OPN localization in the OB at 3, 7, and 21 days post-injury. OPN signal was found predominantly within the EPL and adjacent GL, and within the deeper mitral cell layers (Fig. 4A). Based upon anatomical localization, OPN appeared to be associated with cell bodies and proximal processes of tufted and mitral neurons. These two populations may selectively contain OPN mRNA[60] and are the ORN post-synaptic neurons affected by OB deafferentation. Using IHC for CCK, a marker of tufted cell terminals contacting mitral neurons, we also provided evidence that mitral cells were one of the populations of neurons expressing OPN. Interestingly, OPN tissue expression peaked at 7 days after mFPI, consistent with maximal 48-kD OPN formation, and suggested that these cells may be a source of OPN in this injury model. To probe glial OPN contribution, we performed double-label IHC experiments combining OPN antibody with astrocyte and microglial markers. Unlike other brain regions deafferented by FPI, we found no appreciable OPN protein signal within reactive OB GFAP+ astrocytes or IBA1+ microglia (Fig. 4B).
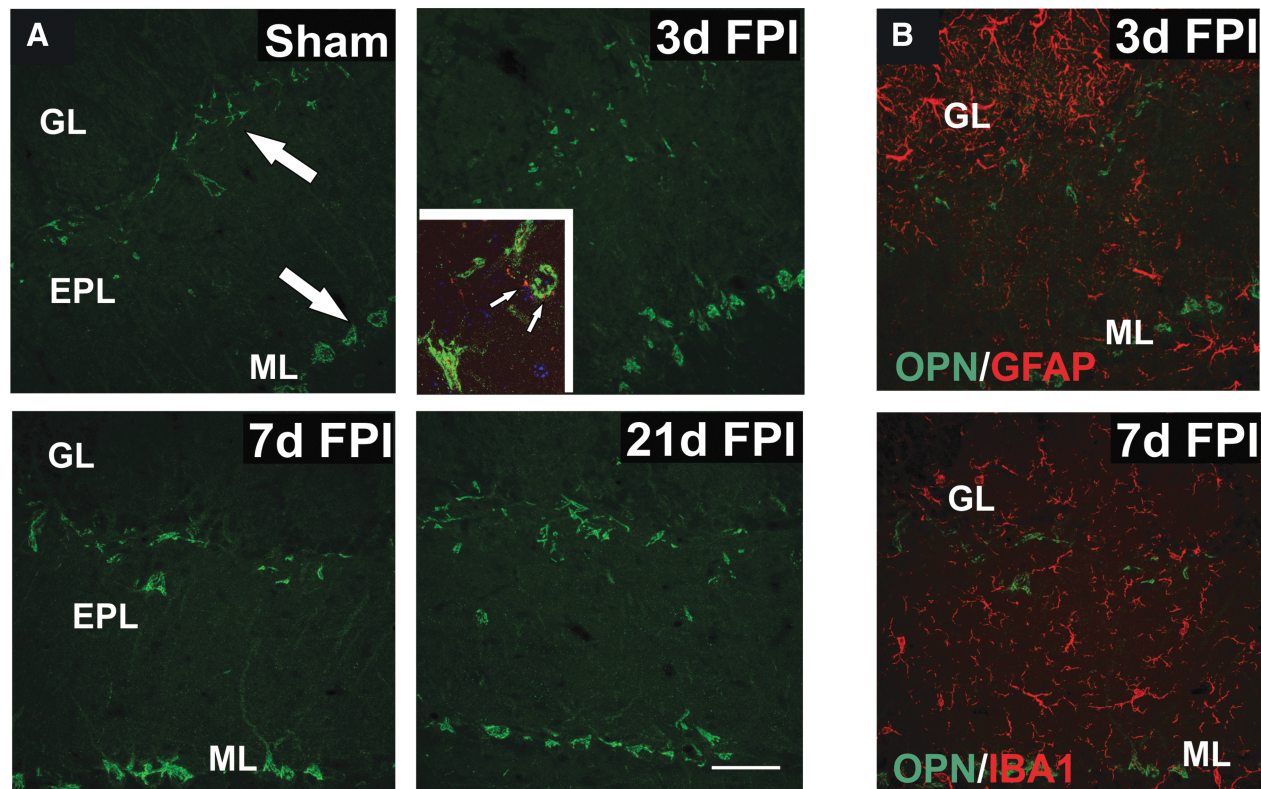
FIG. 4. OPN protein distribution changes within OB after mFPI. (**A**) Imaging of sham cases shows OPN (green) localized to presumptive tufted neurons at the border of GL and EPL, as well as mitral neurons in the ML (arrows). Post-injury OPN signal revealed neuronal increase, modest at 3 days and more robust in cell bodies and primary dendrites at 7 days. At 21 days OPN, intensity appeared to shift toward that of 3-day signal. Inset shows CCK$^+$ terminals (red) of tufted neurons (arrows) surrounding OPN$^+$ mitral cell bodies (green). (**B**) Double label with OPN (green) + GFAP (red) at 3 days and OPN (green) + IBA1 (red) at 7 days failed to show detectable colocalization of signal in reactive glial cells of the deafferented OB. Bar = 50 μm. $n = 3$–4/group. CCK, cholecystokinin; EPL, external plexiform layer; GFAP, glial fibrillary acidic protein; GL, glomerular layer; IBA1, ionized calcium-binding adaptor protein 1; mFPI, mild fluid percussion injury; ML, mitral cell layer; OPN, osteopontin.

Although OPN was observed in OB neuron layers, two aspects of this labeling remained unclear: whether signal represented bound intracellular OPN or secreted protein and whether cells containing OPN at the GL border might include periglomerular neurons. Given that intracellular OPN is reported to be tethered to microtubule-associated proteins,[61] we performed IHC colocalization of OPN and MAP2 to probe for such interaction in tufted and mitral neurons (Supplementary Fig. 1A) (see online supplementary material at http://www.liebertpub.com). Results failed to show OPN colocalization with MAP2, suggesting that OPN within deafferented OB neurons was likely serving a secreted, cell-signaling function. In a second IHC experiment, we paired TH and OPN antibodies, using TH to identify periglomerular inhibitory neurons. Results failed to show colocalization of the two proteins (Supplementary Fig. 1B) (see online supplementary material at http://www.liebertpub.com), indicating that the OPN-positive cells along the GL/EPL border were not inhibitory neurons. Based on TH exclusion, size, and location, we posit that these OPN containing cells are likely local tufted neurons. Future studies utilizing neuronal marker colocalization would confirm this view. Together, these results suggest that deafferented OB neurons direct OPN response after mFPI and that OB glia may be targets of OPN signal peptides generated and released by these neurons.

CD44 receptor expression in olfactory bulb after mild fluid percussion injury

To further explore possible OPN-mediated signaling in response to mFPI, we probed post-injury expression of cell-surface receptor CD44. We posited that CD44 induction would occur in correlation with OPN fragment increase and glial reactivity. Using the same FVB/NJ WT protein extracts, we found significant post-injury elevation in the OB CD44 receptor level at both 3 (364.96 ± 16.96; $p < 0.001$) and 7 days (213.71 ± 61.16; $p < 0.05$) when compared to sham control cases (Fig. 5). Interestingly, this 3-day rise was more than 3-fold and receptor elevation persisted until 7 days. We also observed a trend toward CD44 increase at 1 day (190.41 ± 35.52), but this change failed to reach significance. By 21 days post-injury, CD44 level was equivalent to control (96.77 ± 19.57). Post-hoc analysis confirmed time-dependent differences between 3-day CD44 level and all other time points ($p < 0.01$ for 3 days vs. 1 and 7 days; $p < 0.001$ for 3 vs. 21 days). Acute rise in CD44-mediated signaling is consistent with a reported 3-day peak in CD44/OPN elevation after ischemia[38] and approximates the time course of CD44/OPN change after cryolesion.[37] Here, CD44 expression correlates with OB glial reactivity, peaking at 3 days and returning toward control by 7 days. Although peak CD44 was not entirely synchronous with elevated MMP9 activity and OPN signaling
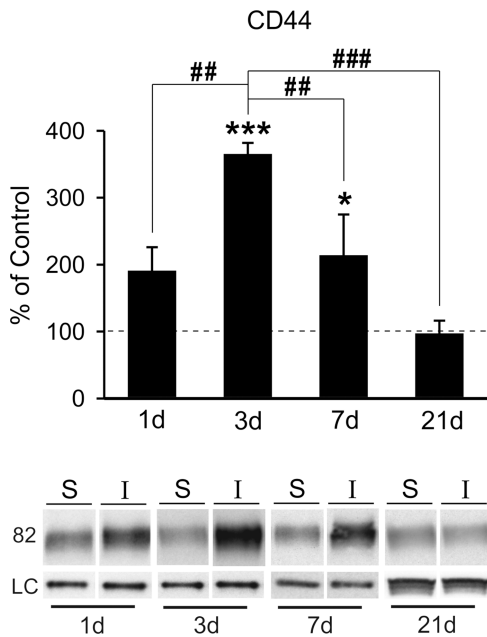
FIG. 5. mFPI increases OB expression of CD44 receptor. (**A**) Post-injury analysis of CD44 protein showed significant elevation of the OPN receptor at 3 and 7 days when compared to sham cases. At 1 day, CD44 trended toward increase, and at 21 days, expression essentially equaled controls. Post-hoc analysis showed the 3-day peak in CD44 protein different from signal at all other time points and confirmed reduction between days 3 and 7. Results are expressed as percent of sham control ROD (100% dashed line). Representative blot images, with cyclophilin A and β-actin load controls, illustrated below. $*p < 0.05$, $***p < 0.001$ versus sham; $^{\#\#}p < 0.01$; $^{\#\#\#}p < 0.001$; $n = 4$–7/group. mFPI, mild fluid percussion injury; OB, olfactory bulb; OPN, osteopontin; ROD, relative optical density.

crease in MMP2 detected in FVB/NJ WT animals. We then proceeded to probe for MMP9 KO effect on the generation of OPN fragments, which were correlated with elevated MMP9 activity at 1 and 7 days post-injury in WT mice. As shown in Figure 6A, loss of MMP9 reduced post-injury 48-kD OPN to levels either equal to
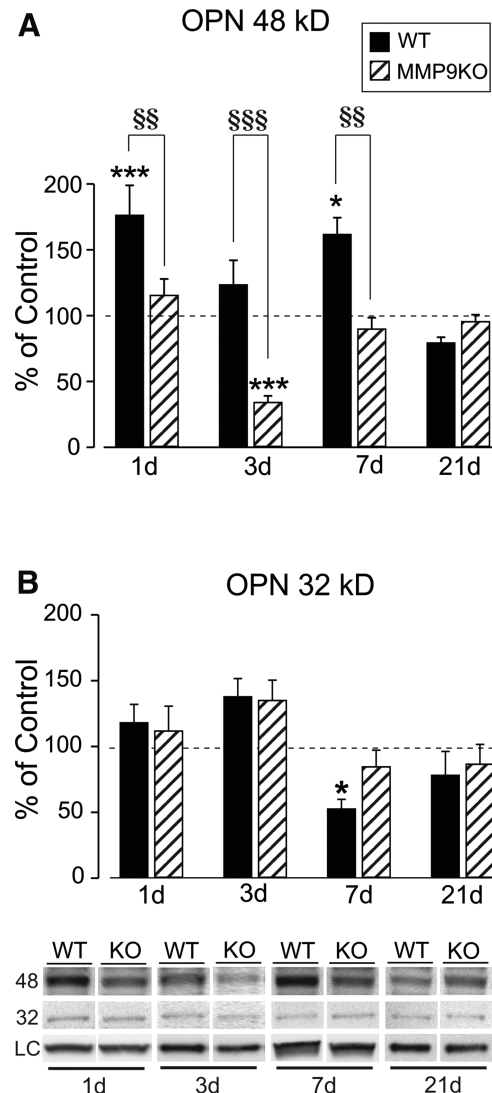
FIG. 6. MMP9 KO alters OPN fragment generation after mFPI. (**A**) Post-injury analysis revealed profound effects of MMP9 KO on 48-kD OPN expression 1–7 days after mFPI. WT elevation of 48-kD OPN at 1 and 7 days (replotted from Fig. 2) was normalized to sham levels in the KO. Loss of MMP9 also reduced 48-kD OPN to 40% of control at 3 days. By 21 days post-injury, MMP9 KO no longer affected 48-kD OPN levels. Post-hoc analysis validated strain differences between 1 and 7 days post-injury. (**B**) Signal for 32-kD OPN in the MMP9 KO was not different from sham controls at any time point, with no post-hoc strain differences detected. MMP9 KO did normalize 7-day 32-kD OPN, suggesting a reduction of 32-kD OPN degradation observed in WT animals. Results are expressed as percent of sham control ROD (100% dashed line). Representative blot images, with cyclophilin A and β-actin load controls, illustrated below. $*p < 0.05$, $***p < 0.001$ versus sham; $^{\S\S}p < 0.01$, $^{\S\S\S}p < 0.001$ WT versus KO; $n = 4$–7/group. KO, knockout; mFPI, mild fluid percussion injury; MMP, matrix metalloproteinase; OPN, osteopontin; ROD, relative optical density; WT, wild type.

fragment generation, we did find upregulation of all three measures at 7 days post-injury. Together, these data suggest a complex interaction between MMP9/OPN/CD44 after FPI, likely facilitating autocrine/paracrine cell signaling.

Matrix metalloproteinase 9 knockout effect on olfactory bulb osteopontin fragments after mild fluid percussion injury

To confirm MMP9/OPN interaction during ORN synaptic repair, we used MMP9 KO mice to test how MMP loss affects OPN lysis and OB synaptic plasticity. Initially, we measured MMP2 activity to assess the extent of compensatory gelatinase response to injury and confirm that KO effects after mFPI result from loss of MMP9. Previous studies of ORN axotomy showed that MMP2 protein was not affected by loss of MMP9.[23] Similarly, we found no compensatory increase of MMP2 activity in MMP9KO mice (Supplementary Fig. 2) (see online supplementary material at http://www .liebertpub.com). At 1, 3, 7, and 21 days post-injury, MMP2 activity in the MMP9 KO was no different from sham controls (103.17 ± 9.47; 119.83 ± 12.15; 113.22 ± 11.82; and 90.38 ± 7.46; $p > 0.05$). Notably, loss of MMP9 attenuated the modest 7-day in-

(115.21 ± 12.58; 89.64 ± 8.69; $p > 0.05$ at 1 and 7 days) or below sham control values (33.99 ± 5.02; $p < 0.001$ at 3 days) between 1 and 7 days post-injury. By 21 days, loss of MMP9 failed to affect 48-kD OPN expression (95.30 ± 5.24). Post-hoc tests revealed striking strain differences at 1, 3, and 7 days post-injury ($p < 0.01$, 1 and 7 days; $p < 0.001$, 3 days). For the 32-kD OPN fragment, we found little evidence of MMP9 KO effect on post-injury response (Fig. 6B). At 1, 3, and 21 days after mFPI, 32-kD OPN in MMP9 KO was not different from FVB/NJ WT injured animals (111.72 ± 18.87; 134.93 ± 15.37; and 86.45 ± 15.07). The one exception was that MMP9 KO normalized 32-kD OPN expression at 7 days (84.49 ± 12.64).

Parallel IHC supported the attenuation of OPN fragment generation observed in MMP9 KO cases. Differences in OPN signal were consistent with reduced 48-kD OPN expression. Specifically, mitral and presumptive tufted neuron labeling at 3 and 7 days post-injury (Fig. 7A,B) was reduced in MMP9 KO relative to WT injured mice, with greatest signal loss in tufted cells at the GL/EPL border 3 days after mFPI. These results show that loss of MMP9 activity significantly attenuates injury-induced 48-kD OPN fragment production and supports the hypothesis that MMP9 activation regulates post-injury cleavage of a critical cell-signaling protein.

Matrix metalloproteinase 9 knockout effect on olfactory bulb synaptic plasticity after mild fluid percussion injury

We next assessed whether MMP9 KO altered postinjury reinnervation of OB synapses by tracking OMP expression, a marker for maturity of ORN axons. Results showed that injury-induced OMP reduction was persistent in MMP9 KO mice (Fig. 8). OMP protein remained below, but was no longer different from, sham-injured controls at 3 days (70.97 ± 9.83; $p > 0.05$). Notably, the ORN axon marker was persistently reduced to 58% and 65% of control values at days 7 (58.94 ± 9.44; $p < 0.05$) and 21 (65.02 ± 7.32; $p < 0.05$), respectively (Fig. 8A). Similar to FVB/NJ WT cases, 1-day OMP signal in the KO was essentially equal to sham control (97.29 ± 9.41; $p > 0.05$). Post-hoc analysis of strain effect further confirmed that OMP remained significantly reduced relative to WT injured cases at both 7 and 21 days after mFPI ($p < 0.05$; $p < 0.01$). We reasoned that persistent reduction of OMP might reflect poor ORN reinnervation and result in aberrant synaptic reorganization for the MMP9 KO. TEM analysis of sham, along with WT and MMP9 KO OB at 21 days post-injury was performed to probe for this possibility. Normal synapto-dendritic morphology re-emerged in 21-day glomeruli of WT mice (Fig. 9A,B), with ORN synapses exhibiting multiple junctional sites and thick post-synaptic densities. By contrast, ORN synapses were poorly developed in glomeruli of injured MMP9 KO mice at 21 days, with less mature post-synaptic density structure (Fig. 9C). More important, 21-day MMP9 KO showed evidence of persistent degeneration, correlating with persistent loss of OMP at this same post-injury interval. These results indicate that MMP9 activity contributes to the time-dependent onset of ORN axon reinnervation after mFPI, possibly involving signal transduction pathways mediated by OPN cell-signaling fragments.
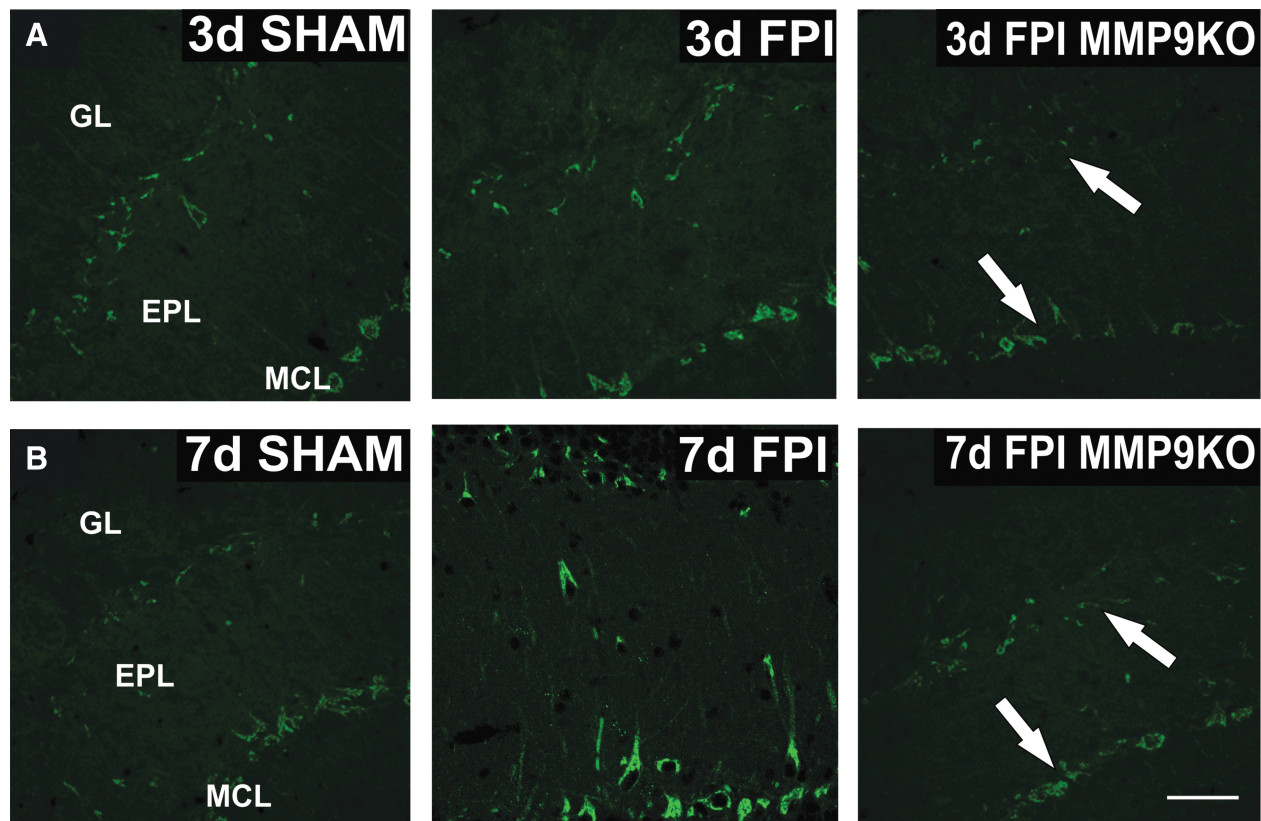
FIG. 7. MMP9 KO alters cellular expression of OPN after mFPI. (**A**) Imaging of sham, WT FPI, and MMP9KO FPI cases at 3 days post-injury shows reduction of OPN labeling in presumptive tufted and mitral neurons of the KO (white arrows) when compared to 3-day WT FPI. (**B**) Strong WT OPN induction at 7 days after FPI relative to sham is also clearly attenuated in the post-injury MMP9 KO. This result is consistent with significant WB loss of 48-kD OPN in the MMP9 KO. Bar = 50 μm; $n = 3–4$/group. EPL, external plexiform layer; GL, glomerular layer; KO, knockout; MCL, mitral cell layer; mFPI, mild fluid percussion injury; MMP, matrix metalloproteinase; OPN, osteopontin; WB, western blot; WT, wild type.

OMP
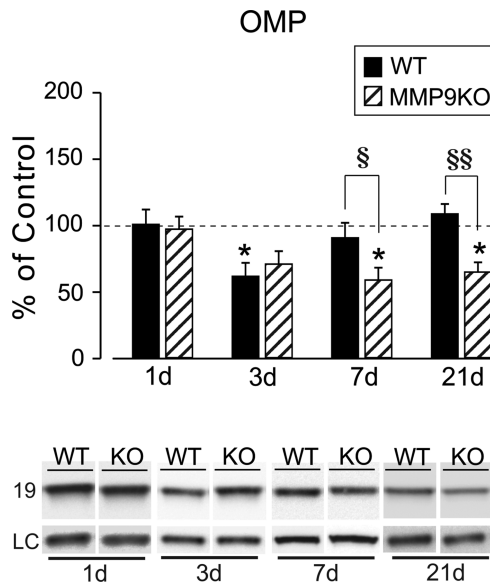
FIG. 8. MMP9 KO alters OMP recovery and synaptic reorganization after mFPI. (**A**) Post-injury analysis revealed that MMP9 KO significantly altered OMP expression. WT 3-day decrease in OMP (replotted from Powell and colleagues,[3] with permission) was attenuated in the KO, no longer different from sham controls. Notably, OMP recovery failed to occur in the MMP9 KO cases at 7 and 21 days, showing persistent reduction from sham levels. This change suggests that loss of MMP9 compromised synaptic recovery and retarded reinnervation. Results are expressed as percent of sham control relative optical density (100% dashed line). Representative OMP images, with β-actin as a load control, illustrated below. *$p < 0.05$ Sham versus TBI; $^{\S}p < 0.05$ WT versus KO; $^{\S\S}p < 0.01$ WT versus KO; $n = 4–7$/group. KO, knockout; mFPI, mild fluid percussion injury; MMP, matrix metalloproteinase; OMP, olfactory marker protein; TBI, traumatic brain injury; WT, wild type.

CD44 protein and astrocyte reactivity in the matrix metalloproteinase 9 knockout after mild fluid percussion injury

As for FVB/NJ WT, we assessed CD44 protein in the OB of injured MMP9 KO mice. Loss of MMP9 failed to change the time course of CD44 protein expression after mFPI (Fig. 10). At 1 and 21 days after injury, CD44 protein of injured MMP9 KO mice was not different from sham controls (131.57 ± 11.30; 90.29 ± 10.32; $p > 0.05$). As for injured WT mice, the OPN receptor in MMP9 KO remained significantly elevated over sham cases at 3 and 7 days post-injury (267.77 ± 33.03, $p < 0.001$; 247.68 ± 35.95, $p < 0.001$). This was confirmed with post-hoc analysis, which showed no strain differences at any time point. Given that MMP9 was elevated in reactive, GFAP+ astrocytes (see again, Fig. 2), we conducted IHC to determine whether loss of MMP9 affects these cells. Astrocyte CD44 receptors can interact with OPN to mediate paracrine signaling,[35] suggesting that attenuated OPN expression in the KO might affect glial reactivity. This reactivity is critical to clearance of degenerating axons, as well as growth factor induction for synaptic regeneration. As for CD44, MMP9 loss did not alter GL astrocyte response, where cell morphology was not different from WT at either 3 or 7 days post-injury (Supplementary Fig. 3A,B)

(see online supplementary material at http://www.liebertpub.com). Such results suggest that MMP9's role in glial reactivity might be redundant, allowing for compensation by other intact enzyme systems. Thus, post-injury rise in CD44 does not appear to be dependent upon MMP9 or specific MMP9/OPN signaling. The result also points to OPN action through alternative receptor populations (e.g., vitronectin, $\alpha_v\beta_3$ integrin receptors), perhaps supporting persistent CD44 activation in the MMP9 KO after mFPI.

Discussion

This study mapped OB post-injury MMP9 activation and OPN expression in the FVB/NJ mouse subjected to mFPI, an insult generating diffuse ORN axotomy and reactive synaptogenesis.[3] Given that ORN ablation and axon transection induce gelatinases,[22,23,62] and MMP activation cleaves the cytokine, OPN, in other brain regions,[9] we posited that mFPI of the OB would generate time-dependent MMP9 activity, OPN signaling fragment production, and increase of CD44 OPN receptor. To further test this interaction, a cohort of MMP9 KO mice was subjected to mFPI, then probed for OPN fragments and assayed ORN terminal regeneration. We report paired post-injury activation of MMP9 and expression of OPN RGD signaling fragments. Time-dependent increase in CD44 receptor also occurred, but was delayed relative to MMP9 activation and OPN fragment production. Post-injury MMP9 protein was elevated in reactive astrocytes and post-synaptic neurons, but OPN was localized to deafferented mitral and tufted neurons. Moreover, OPN failed to show cytoskeletal colocalization consistent with its restricted intracellular isoform and was not present within periglomerular inhibitory neurons. Importantly, MMP9 KO mice did not show post-injury increase of OPN fragments, supporting MMP9/OPN interaction after mFPI. Loss of MMP9 also reduced OPN localization within presumptive tufted and mitral neurons, revealed persistent reduction of ORN axon marker OMP, along with attenuated synaptic recovery. These results reveal the time course of OB response to diffuse, mild FPI and identify mediators of synaptic repair. We conclude that cell-signaling pathways, supported by interaction between MMP9, OPN, and CD44, are critical to post-injury OB synapse recovery.

Olfactory bulb gelatinase activity shows time-dependent change after mild fluid percussion injury

We first assessed OB MMP2 and MMP9 activity during both degenerative and regenerative post-injury phases (1–21 days). These gelatinases are produced by neurons and glia,[5,6] contributing to both injury pathology and regenerative response.[64] Here, we report time-dependent elevation in gelatinase activity after mild, diffuse injury of the OB, with MMP9 activity induced earlier and to a greater extent than MMP2. This pattern is consistent with the time course of OB enzyme expression after ORN transection or nasal epithelium ablation,[21–23] where MMP9 peaked during axon degeneration and MMP2 with subsequent axon/synapse recovery. A similar time course of enzyme response is also documented for other brain regions affected by traumatic injury. For example, MMP9 activity is maximal at early degenerative periods after hippocampal deafferentation, whereas MMP2 response evolves later, during axonal sprouting and synapse reformation.[5,7] This MMP role separation is supported by the observation that MMP2 promotes axon regeneration in the presence of primary olfactory
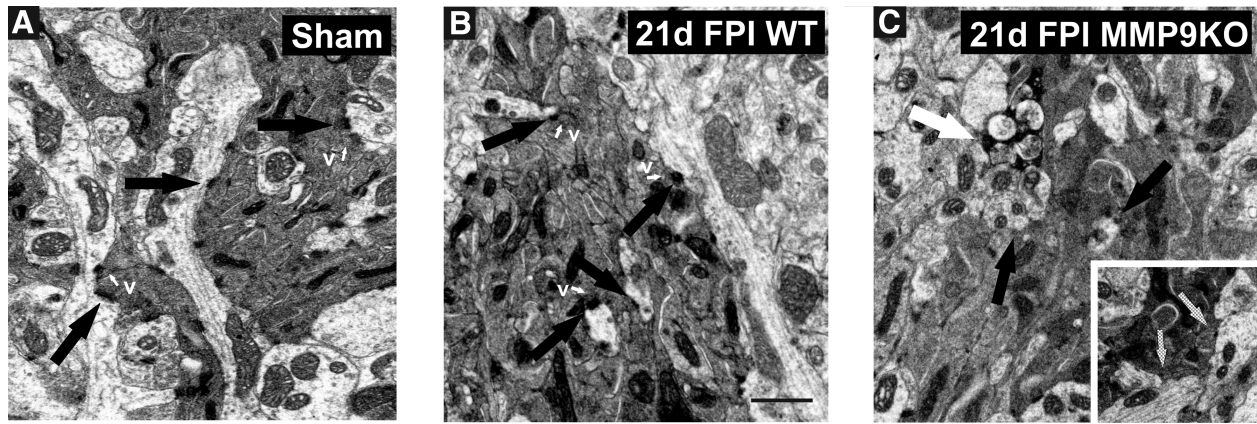
FIG. 9. MMP9 KO attenuates synaptic repair at 21 days after mFPI. (**A**) Sham OB illustrates glomerular dendrites, well-formed synaptic junctions with electron dense afferent ORN axons (black arrows) and adjacent synaptic vesicles (v; white arrows). (**B**) At 21 days after mFPI, WT mice showed reorganization of pre-synaptic ORN axon terminals with synaptic vesicles (v; white arrows), well-defined synaptic junctions, and thick post-synaptic densities (black arrows). (**C**) In the 21-day postinjury MMP9 KO, synaptic junctions are loosely formed (black arrows; hatched arrows inset), with diffuse pre-synaptic vesicles and sites of active degeneration (white arrow). Bar = 1 μm; $n = 3$/group. KO, knockout; mFPI, mild fluid percussion injury; MMP, matrix metalloproteinase; OB, olfactory bulb; ORN, olfactory neuron; WT, wild type.
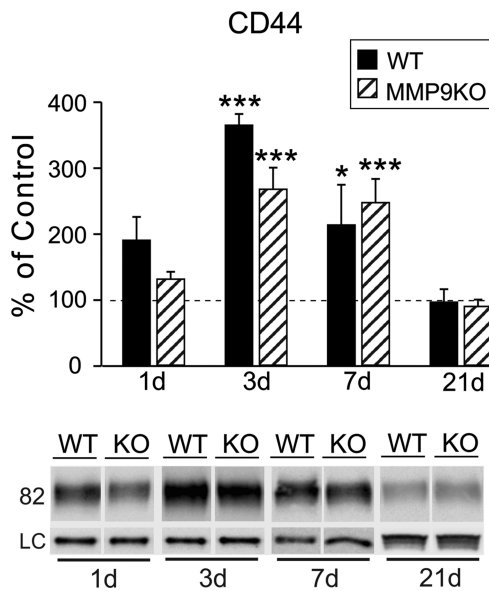
FIG. 10. Loss of MMP9 does not affect CD44 expression after mFPI. Post-injury analysis of OB CD44 showed significant elevation at both 3 and 7 days in the MMP9 KO, similar to the profile observed in WT injured cases (replotted from Fig. 5). No strain differences were detected in post-hoc analysis. Similarly, injury did not change CD44 protein at either 1 or 21 days in the KO. Results are expressed as percent of sham control ROD (100% dashed line). Representative CD44 blot images, with cyclophilin A and β-actin load controls, illustrated below. $*p < 0.05$, $***p < 0.001$ vs. sham; $n = 3$–5/group. KO, knockout; mFPI, mild fluid percussion injury; MMP, matrix metalloproteinase; OB, olfactory bulb; ROD, relative optical density; WT, wild type.

ensheathing cells[65] and, more recently, was found important to successful neuronal maturation during development of cognitive and motor function.[66] Despite similarities to other brain regions, OB MMP response was different in two important aspects: predominant biphasic MMP9 activation and significant upregulation of MMP9 within both glia and neurons. First, we found MMP9 activity dominated in the injured OB, with significant increase in activity at both acute and subacute intervals. Further, MMP9 activity returned to control level by 21 days after mFPI, quite different from both olfactory nerve transection and OE ablation, where MMP9 protein remained elevated throughout the 15- to 35-day postinjury period.[21,23] Considering that reactive synaptogenesis in the OB is delayed relative to other brain regions,[54] this biphasic pattern of MMP9 activity suggests a secondary role for the enzyme during the period of axon degeneration. It is also interesting that we observed two similar peaks in MMP9 activity after a rather mild insult, whereas one acute peak in MMP9 protein typically occurs after the more-severe, full transection of the olfactory nerve.[23] This raises the possibility that separate periods of MMP9 activity may be required for the evolution of synaptic pathology/recovery induced by diffuse axon injury. Indeed, we have recently documented that diffuse mFPI appears to involve different types synaptic insult, requiring both *de novo* synaptic reconstruction, as well as more simple reshaping of intact synapses.[3] Perhaps a different synaptic modification is required after diffuse brain insult, where type or extent of remodeling dictates more complex MMP activity.

A second difference in OB MMP response was detected with IHC, where the enzyme was upregulated not only in reactive astrocytes, but also within GL and EPL neurons. Notably, this increase in MMP9 labeling matched post-injury intervals of peak OB enzyme activity. Reactive glia are a principal source of inducible MMPs around cortical synapses deafferented by traumatic brain injury[17,67,68] or synapses targeted by entorhinal lesion.[5,15] After olfactory nerve transection, Costanzo and colleagues[22] found MMP9 elevation correlated with increased GFAP expression, suggesting reactive astrocytes as a principal source of MMP9 with OB deafferentation. However, after diffuse OB injury, we observed

MMP9 increase within both glia and deafferented neurons of the GL. Neurons affected by the injury appear to take an active role in directing MMP9 response. It is possible that this pattern results from a more focused and local synaptic repair rather than regeneration of the entire olfactory nerve input. Thus, local repair could not only involve glial modification of the synaptic environment, but also a more fine-tuned plasticity required within the post-synaptic neurons. If MMP9 facilitates molecular signaling for such plasticity, then its induction after mFPI would be expected to be different from continuous activation after ORN axotomy. Indeed, Bakos and Costanzo[62] reported that continuous MMP9 upregulation correlates with invading neutrophils after full transection of the olfactory nerve, suggesting that persistent inflammation after severe injury may drive ongoing enzyme activation. In contrast to MMP9, we observed only minor post-injury effects on MMP2 activity, suggesting its modest induction after mFPI, unlike the pronounced MMP2 protein elevation reported after ORN axotomy.[23] If MMP2 promotes axon regeneration and synaptic reconstruction, it is reasonable to predict a reduced MMP2 response in the absence of massive axon damage with mFPI. Overall, the present study reveals a time-dependent induction of MMP9 activity, which may target critical molecular substrates to facilitate removal of degenerative debris and promote the onset of synaptic repair. OPN is potentially one such target.

Osteopontin cell signaling fragments increase after mild fluid percussion injury

MMP cleavage of the RGD/SVVYGLR sequence within OPN generates 48- and 32-kD signaling fragments,[31,32,34,69] peptides which are elevated after central nervous system (CNS) deafferentation,[9] and drive cell activation during the inflammatory response.[70] These peptides bind to both integrin and CD44 receptors, directing cell adhesion and migration.[34,71] In the present study, we provide evidence that 48-kD OPN is the prominent functional fragment induced by diffuse OB deafferentation. As predicted from other CNS insults,[9,72] maximal 48-kD OPN signal occurred at 1 day post-injury, consistent with acute inflammatory signaling. Typically, acute OPN signaling returns to baseline within a week after insult.[9,36,37,73] Here, we found an unexpected second rise of 48-kD OPN production at 7 days after mFPI. Moreover, each OPN fragment peak was correlated with increased MMP9 activity, suggesting a direct enzyme/substrate interaction. Similar interaction was probed after hippocampal deafferentation, where pharmacological inhibition of MMP9 activity attenuated 48-kD OPN.[9] Given the evidence for ORN terminal damage and OB synapse reorganization after mFPI,[3] it is possible that 48-kD OPN directs not only acute inflammatory signals for glial activation and debris removal, but also primes the neuropil for re-establishment of local synapses. Notably, OB glial reactivity is reduced by 21 days post-injury,[3] a time point where both MMP9 activity and 48-kD OPN fragment generation return to baseline. Tandem increase in MMP9 and OPN expression also occurs with axon pathology of cortical deafferentation[5] and in multiple sclerosis, where patient C-C chemokine receptor (CCR)2$^+$/CCR5$^+$ T cells can produce high levels of both proteins.[74] The present study also detected a reduction in 32-kD OPN correlated with the second period of elevated MMP9 activity. Such reduction is consistent with reports that MMP9 supports additional 32-kD proteolysis during recycling of the C-terminal fragment.[31,32]

Although we found OPN localized within mitral and presumptive tufted neurons, questions remain as to where the cytokine is processed within the deafferented OB. Other studies show OPN localized within both neurons[37] and glia[75–77]; however, after CNS injury, OPN transcript is prominent within microglia and elevated protein found in both microglia and astrocytes.[9] In our study, OPN was not detectable within OB astrocytes and microglia, but appeared upregulated in ORN postsynaptic neurons, suggesting a response selective for the principal deafferented cells. Further, OPN signal was greatest at 7 days, matching peak MMP9 activity and 48-kD OPN generation. To our knowledge, such neuronal OPN response is unique among cortical regions affected by TBI, suggesting that injury-induced secretion of OPN might originate within the deafferented neurons themselves. Given that OPN can exist as a cytoplasmic isoform (OPN$_i$) that binds to microtubule associated proteins,[61] we explored whether this neuronal signal reflected OPN$_i$. Based on the absence of OPN$_i$/MAP2 colocalization, we conclude that OB OPN is likely functioning as a neuron secreted or receptor-bound form affecting surrounding cells.[60,78] It is also possible that OPN labeled cells might include periglomerular inhibitory neurons affected by ORN axon damage. However, we failed to find OPN colocalized with their marker protein tyrosine hydroxylase, making it unlikely that inhibitory neurons contribute to post-injury OPN upregulation. Together, our results reveal an ordered OPN processing within the diffusely injured OB, where fragment generation is correlated with significant elevation in MMP9 activity. This response appears to originate within the deafferented neurons, leading to a rise in OPN signaling peptides that direct synaptic repair.

Osteopontin receptor CD44 is elevated after mild fluid percussion injury

Our results show time-dependent change in the generation of 48- and 32-kD OPN after mFPI. These peptides have a high affinity for integrin and CD44 receptors, which direct inflammatory activation, migration, and axon growth.[34,71,79] Indeed, antibodies to integrin β_1 and CD44 block OPN-mediated neurite outgrowth,[79] and manipulation of Rac family small GTPase 1/protein kinase N gamma alters CD44-mediated astrocyte reactivity and migration.[80] We focused on CD44 because it is acutely elevated over perilesional areas[39] and increases within activated microglia and macrophages.[77] In the OB, CD44 receptor showed time-dependent elevation after mFPI, peaking at 3 days, with persistent, yet lower, elevation at 7 days post-injury. The fact that the peak CD44 increase was delayed relative to the initial 1-day rise of 48-kD OPN signal demonstrates acute asynchrony between induction of CD44 and its potential ligand. By contrast, the later 7-day OPN elevation was matched by a CD44 increase, indicative of typical injury-induced receptor/ligand binding. These differences suggest that OPN may influence CD44 signaling by both indirect and direct interaction after mFPI. One explanation for the acute asynchrony would be that OPN signals receptor upregulation, which then peaks later. This scenario is plausible given that CD44 membrane expression increases in the presence of OPN, and OPN is posited to facilitate CD44 phosphorylation, which permits receptor binding to MMP9 and regulation of enzyme activity.[81] Such MMP9 activation could then potentiate OPN signaling and effects on synaptic plasticity. Our results also suggest that CD44 receptor role is greater during the subacute degeneration phase given that its expression is normalized by the 3-week onset of active reinnervation.

A similar temporal pattern of CD44 increase and decline was reported after central and peripheral nerve transection.[82] However, in these cases, CD44 induction within reactive glia appeared to be

driven by general cell damage, blood–brain barrier disruption or leukocyte infiltration through intact vascular interfaces. In these models, the receptor was posited to facilitate cell adhesion by binding with matrix molecules such as hyaluronate, fibronectin, collagen IV, laminin, and chondroitin sulphate. It is likely that OB glial reactivity after mFPI also includes CD44-mediated interaction with these matrix proteins to alter cell adhesion and mobility. Thus, it is possible that CD44 receptor expression responds independently of MMP9/OPN in the injured OB; however, the correlation of OPN fragment generation and glial cellular reactivity argues for OPN/CD44 interaction. For example, we observed a common peak in glial reactivity and CD44 response at 3 days after mFPI. This pattern also matches the post-ischemia profile proposed by Kang and colleagues,[38] where microglial activation at 2–3 days post-injury mediates glial mobility and cell adhesion through CD44 pathways. Thus, it appears that OPN/CD44 signaling contributes to the timing of successful OB synaptic repair. Interestingly, 32-kD OPN, which also binds CD44, may oppose 48-kD OPN/CD44 receptor-driven adhesion, providing a means to balance growth at different stages of the degeneration/regeneration cycle.[83–85] Future studies probing OPN selective $\alpha_V\beta_3$ integrin receptor will help determine the relative contribution of the two OPN signaling pathways within the injured OB.

Matrix metalloproteinase 9 knockout reverses mild fluid percussion injury generation of osteopontin proteolytic fragments

In the first part of this study, we observed a direct correlation between post-injury MMP9 activity and production of OPN-signaling peptides. Proof of MMP9 and OPN interaction was tested using homozygous MMP9 KO mice generated on the same FVB/NJ background.[23] Whereas other systemic insults, such as kidney obstruction disease, have linked MMP9 inhibition with reduction in OPN cleavage,[33] the present study is the first to explore OPN fragment generation in MMP9 KO mice subjected to mFPI. Loss of MMP9 had significant effect on both 48- and 32-kD OPN. Foremost, 48-kD OPN returned to control expression. Such normalization supports MMP9/OPN interaction as the source for a key OPN-signaling peptide within the injured OB. Interestingly, MMP9 KO also reduced 48-kD OPN below control level at 3 days post-injury, a result more difficult to interpret. It appears that without MMP9, either the 48-kD OPN lytic site is less targeted or other proteases[34] are more efficient at further degrading the fragment. We also found that MMP9 KO affected 32-kD OPN at 7 days after mFPI, where loss of enzyme reversed WT reduction of this carboxy terminal fragment. Given that MMP9 can act to degrade OPN carboxy terminal peptides for recycling,[34] it is possible that 32-kD OPN expression shifts toward control level in the KO. Alternatively, the observed KO differences in 32-kD OPN could be produced through activation of gelatinase homologue MMP2 or other proteases (e.g., other MMPs, thrombin[34]). We believe this interpretation is less likely, given that no strain differences in OB MMP2 activity were observed and we failed to detect KO differences for either OPN fragment when compared to sham control cases at the remaining time points. In further support of MMP9/OPN interaction, we found OPN reduction in both presumptive tufted and mitral neurons of the injured MMP9KO, consistent with the significant drop in 48-kD OPN. Together, the effect of MMP9 KO on the two OPN fragments represents a novel, multi-phasic role for MMP9 in the generation of OPN signaling during OB axon degeneration and synaptic regeneration. This is in contrast to the majority of CNS insults, where MMP9 induction is acute, peaking well before onset of regeneration.[5,23,67,68]

Post-injury reduction of OPN fragments in the MMP9 KO suggests that upregulation of CD44 might also be attenuated. Surprisingly, we failed to observe this effect. Though trending lower, the two CD44 peaks in expression for the MMP9 KO were not different from WT. This suggests that CD44 signaling after OB injury is not dependent on MMP9, and that 48-kD OPN generated by MMP9 may represent a pool acting through other receptor pathways (e.g., integrin receptor binding). Alternatively, it has been reported that a reduction of cleaved OPN increases CD44 membrane deposition.[81] Thus, it is possible that lower expression of 48-kD OPN in the KO could contribute to the maintenance of CD44 protein after mFPI. Further, CD44 receptor levels might also be retained by compensatory activation of other MMPs. For example, MT-1 MMP targets membrane-tethered CD44, cleaving the receptor's intracellular domain, which then acts as a transcription factor for CD44 mRNA upregulation.[86] Given that OPN localizes in presumptive tufted and mitral cells, it seems likely that OPN regulation of CD44 signaling occurs within injured OB neurons. Although we did not perform CD44 IHC, we have found the receptor expressed in both neurons and glia of other cortical regions subjected to mFPI (Powell, Doperalski, and Phillips, unpublished results). Given that post-injury glial activation can occur through CD44 receptors,[37,38,82] and receptor protein did not change in the MMP9KO, it follows that astrocyte/microglial reactivity may not be affected in the KO, which we did observe. In fact, post-injury OB glial phenotype could be maintained by CD44, through interaction with inflammatory cytokines tumor necrosis factor alpha and interleukin-1 beta.[87,88] Interestingly, a recent report using the ORN transection model showed subacute dexamethasone modulation of OB inflammation during the post-injury period, where we observed peak CD44 induction, improved olfactory outcome.[89] Together, these results support a complex OPN/receptor interaction within the post-injury OB. Given CD44 stability in MMP9 KO mice, it will be important to map the OPN $\alpha_V\beta_3$ integrin receptor after mFPI, with the goal of better defining the role of different OPN fragments generated by MMP9.

Matrix metalloproteinase 9 knockout attenuates recovery of olfactory neuron axons and olfactory bulb synaptic reorganization after mild fluid percussion injury

A number of studies have used OMP as an index of ORN axon maturity during development and OB reinnervation after injury.[90–92] Loss of OMP at 3 days after mFPI confirmed diffuse axon damage in the OB[3]; however, this reduction was attenuated relative to severe ORN insults,[21,22,92] and returned to control baseline earlier, indicating a more rapid reinnervation. To clarify whether or not MMP9/OPN signaling impacts this ORN terminal loss or recovery, we probed OMP expression within injured MMP9 KOs. Surprisingly, loss of MMP9 caused a persistent OMP reduction, extending to both 7 and 21 days post-injury, time points where even WT models of severe ORN lesion show protein recovery.[21,22,92,93] In fact, this persistent OMP loss in the KO was correlated with 7-day reduction of 48-kD OPN, supporting the hypothesis that OPN cell signaling is critical to the onset of ORN reinnervation.

To further identify MMP9KO effect on this reinnervation, glomerular ultrastructure was examined at 21 days after mFPI and directly compared to WT cases, where OMP is normalized and active synaptic regeneration occurs.[3] This time frame matches that for establishment of ORN/mitral and ORN/tufted excitatory

synapses,[94,95] and the reinnervation of asymmetric ORN synapses as confirmed by post-synaptic wheat germ agglutinin/HRP labeling.[54] In line with the persistent post-injury OMP reduction and reduced OPN fragment production, we failed to observe ORN synaptic recovery in MMP9 KO. Axon degeneration and synaptic disruption remained, along with poorly organized junctions, thin post-synaptic densities, as well as disrupted cytoskeleton and pre-synaptic vesicles. To our knowledge, only one other study[23] examined effects of MMP9 KO on OB injury response, utilizing the full ORN transection model. Whereas that study did not include ultrastructural analysis, the researchers report that MMP9 KO failed to affect time-dependent MMP2 induction, which they previously correlated with onset of ORN reinnervation, nor did it affect progress of recovery. Thus, it would appear that the time-dependent ORN terminal degeneration and synaptic reinnervation after diffuse brain injury may be more sensitive to the loss of MMP9. We conclude that loss of MMP9-associated OPN signaling in the KO curtails glial clearance of damaged ORN axon terminals and impairs reinnervation, which can be mapped by persistent post-injury reduction of OMP.

These effects of MMP9 KO on OMP and synaptic plasticity could be attributed to loss of injury-induced OPN fragments responsible for glial activation in response to ORN axon damage. Such glial activation has been documented after ischemia,[38] cortical stab wound,[37] and hippocampal deafferentation.[9] Persistent degenerative debris would affect ECM reorganization and prolong onset of ORN reinnervation. In addition, MMPs target molecules that stabilize synaptic junctions[15,96,97] and vascular endothelium.[98] Loss of MMP9 likely alters these processes in the OB, delaying preparation of the local synaptic environment for post-injury reorganization.

Alternatively, loss of MMP9/OPN signaling might also affect axonal regrowth and synapse regeneration, here marked by a persistent OMP deficit. Axon sprouting and elongation are linked to OPN, as well as extent of CNS cell migration, principally shown in glioma[99] and astrocytoma[100] models. Loss of OPN at a critical point in axonal migration could delay maturation of ORN axons with OMP. Further, *in vitro* studies also link MMP9 to α-tubulin organization in growing neurites, defining an enzymatic role during axonal elongation.[101] Although no previous studies of TBI plasticity use MMP9 KO mice to define MMP9/OPN interaction, studies with cortical barrel field insult and monocular deprivation have examined sensory axonal plasticity in MMP9 KOs. Results from these studies support our OB findings. Kaliszewska and colleagues[45] reported that loss of MMP9 caused significant decrease in experience-dependent synaptic plasticity within barrel fields of cortical layers II–IV. After monocular deprivation, ocular dominance plasticity was mapped in MMP9 KO mice, with KO causing a clear reduction of spine and synapse density within visual cortex.[102] Collectively, experiments with MMP9 KO reported here support the hypothesis that MMP9-generated 48-kD OPN signal influences the time course of ORN axon sprouting and glomerular synaptic plasticity.

Conclusions

The present study documents time-dependent gelatinase activation, OPN proteolysis, and CD44 receptor upregulation within the deafferented OB after diffuse mFPI. An enzyme/substrate interaction between MMP9 and OPN is supported, generating a 48-kD OPN peptide to facilitate both early degenerative and subsequent regenerative phases of synaptic plasticity. OB postinjury OPN sig-

nal is generated within deafferented tufted and mitral neurons, not in reactive glia or periglomerular inhibitory neurons. The importance of MMP9 in supporting OB synaptic plasticity is confirmed with KO mice, where loss of the enzyme prevents 48-kD OPN elevation and promotes persistent ORN axon damage to delay synaptic regeneration.

Author Disclosure Statement

No competing financial interests exist.

References

1. Steward, O. (1989). Reorganization of neuronal connections following CNS trauma: principles and experimental paradigms. J. Neurotrauma 6, 99–152.
2. Oley, N., DeHan, R.S., Tucker, D., Smith, J.C., and Graziadei, P.P. (1975). Recovery of structure and function following transection of the primary olfactory nerves in pigeons. J. Comp. Physiol. Psych. 88, 477–495.
3. Powell M.A., Black, R.T., Smith, T.L., Reeves, T.M., and Phillips, L.L. (2017). Mild fluid percussion injury induces diffuse axonal damage and reactive synaptic plasticity in the mouse olfactory bulb. Neuroscience 317, 106–118.
4. Frischknecht, R., and Gundelfinger, E.D. (2012). The brain's extracellular matrix and its role in synaptic plasticity. Adv. Exp. Med. Biol. 970, 153–171.
5. Phillips, L.L., Chan, J.L., Doperalski, A.E., and Reeves, T.M. (2014). Time-dependent integration of matrix metalloproteinases and their targeted substrates directs axonal sprouting and synaptogenesis following central nervous system injury. Neural Regen. Res. 9, 362–376.
6. Wlodarczyk, J., Mukhina, I., Kaczmarek, L., and Dityatev, A. (2011). Extracellular matrix molecules, their receptors, and secreted proteases in synaptic plasticity. Dev. Neurobiol. 71, 1040–1053.
7. Phillips, L.L., and Reeves, T. M. (2001). Interactive pathology following traumatic brain injury modifies hippocampal plasticity. Restor. Neurol. Neurosci. 19, 213–235.
8. Kim, H.J., Fillmore, H.L., Reeves, T.M., and Phillips, L.L. (2005). Elevation of hippocampal MMP-3 expression and activity during trauma-induced synaptogenesis. Exp. Neurol. 192, 60–72.
9. Chan, J.L., Reeves, T.M., and Phillips, L.L. (2014). Osteopontin expression in acute immune response mediates hippocampal synaptogenesis and adaptive outcome following cortical brain injury. Exp. Neurol. 261,757–771.
10. Dityatev, A., Dityateva, G., Sytnyk, V., Delling, M., Toni, N., Nikonenko, I., Muller, D., and Schachner, M. (2004). Polysialylated neural cell adhesion molecule promotes remodeling and formation of hippocampal synapses. J. Neurosci. 24, 9372–9382.
11. Falo, M.C., Reeves, T.M., and Phillips, L.L. (2008). Agrin expression during synaptogenesis induced by traumatic brain injury. J. Neurotrauma 25, 769–783.
12. Harris, J.L., Reeves, T.M., and Phillips, L.L. (2011). Phosphacan and receptor protein tyrosine phosphatase beta expression mediates deafferentation-induced synaptogenesis. Hippocampus 21, 81–92.
13. Harris, N.G., Mironova, Y.A., Hovda, D.A., and Sutton, R.L. (2010). Chondroitinase ABC enhances pericontusion axonal sprouting but does not confer robust improvements in behavioral recovery. J. Neurotrauma 27, 1971–1982.

14. Mahmood, A., Wu, H., Qu, C., Mahmood, S., Xiong, Y., Kaplan, D. L., and Chopp, M. (2014). Suppression of neurocan and enhancement of axonal density in rats after treatment of traumatic brain injury with scaffolds impregnated with bone marrow stromal cells. J. Neurosurgery 120, 1147–1155.

15. Warren, K.M., Reeves, T.M., and Phillips, L.L. (2012). MT5-MMP, ADAM-10, and N-cadherin act in concert to facilitate synapse reorganization after traumatic brain injury. J. Neurotrauma 29, 1922–1940.

16. Yamaguchi, Y. (2001). Heparan sulfate proteoglycans in the nervous system: their diverse roles in neurogenesis, axon guidance, and synaptogenesis. Semin. Cell Dev. Biol. 12, 99–106.

17. Wang, X., Jung, J., Asahi, M., Chwang, W., Russo, L., Moskowitz, M.A., Dixon, C.E., Fini, M.E., and Lo, E.H. (2000). Effects of matrix metalloproteinase-9 gene knock-out on morphological and motor outcomes after traumatic brain injury. J. Neurosci. 20, 7037–7042.

18. Hsu, J.Y., McKeon, R., Goussev, S., Werb, Z., Lee, J.U., Trivedi, A., and Noble-Haeusslein, L. J. (2006). Matrix metalloproteinase-2 facilitates wound healing events that promote functional recovery after spinal cord injury. J. Neurosci. 26, 9841–9850.

19. Hsu, J.Y., Bourguignon, L.Y., Adams, C.M., Peyrollier, K., Zhang, H., Fandel, T., Cun, C.L., Werb, Z., and Noble-Haeusslein, L.J. (2008). Matrix metalloproteinase-9 facilitates glial scar formation in the injured spinal cord. J. Neurosci. 28, 13467–13477.

20. Verslegers, M., Lemmens, K., Van Hove, I., and Moons, L. (2013). Matrix metalloproteinase-2 and -9 as promising benefactors in development, plasticity and repair of the nervous system. Prog. Neurobiol. 105, 60–78.

21. Bakos, S.R., Schwob, J.E., and Costanzo, R.M. (2010). Matrix metalloproteinase-9 and -2 expression in the olfactory bulb following methyl bromide gas exposure. Chem. Senses 35, 655–661.

22. Costanzo, R.M., Perrino, L.A., and Kobayashi, M. (2006). Response of matrix metalloproteinase-9 to olfactory nerve injury. Neuroreport 17, 1787–1791.

23. Costanzo, R.M., and Perrino, L.A. (2008). Peak in matrix metalloproteinases-2 levels observed during recovery from olfactory nerve injury. Neuroreport 19, 327–331.

24. de Castro, R.C, Jr, Burns, C.L., McAdoo, D.J., and Romanic, A.M. (2000). Metalloproteinase increases in the injured rat spinal cord. Neuroreport11, 3551–3554.

25. Horstmann,S., Su, Y., Koziol, J., Meyding-Lamade, U., Nagel, S., and Wagner, S. (2006). MMP-2 and MMP-9 levels in peripheral blood after subarachnoid hemorrhage. J. Neurol. Sci. 251, 82–86.

26. Noble, L.J., Donovan, F., Igarashi, T., Goussev, S., and Werb, Z. (2002). Matrix metalloproteinases limit functional recovery after spinal cord injury by modulation of early vascular events. J. Neurosci. 22, 7526–7535.

27. Hashimoto, M., Sun, D., Rittling, S.R., Denhardt, D.T., and Young, W. (2007). Osteopontin-deficient mice exhibit less inflammation, greater tissue damage, and impaired locomotor recovery from spinal cord injury compared with wild-type controls. J. Neurosci. 27, 3603–3611.

28. Jin, Y., Kim, I.Y., Kim, I.D., Lee, H.K., Park, J.Y., Han, P.L., Kim, K.K., Choi, H., and Lee, J.K. (2014). Biodegradable gelatin microspheres enhance the neuroprotective potency of osteopontin via quick and sustained release in the post-ischemic brain. Acta Biomaterialia 10, 3126–3135.

29. Miyazaki, K., Okada, Y., Yamanaka, O., Kitano, A., Ikeda, K., Kon, S.,Uede, T., Rittling, S.R., Denhardt, D.T., Kao, W.W., and Saika, S. (2008). Corneal wound healing in an osteopontin-deficient mouse. Invest. Ophthalmol. Vis. Sci. 49, 1367–1375.

30. Topkoru, B.C., Altay, O., Duris, K., Krafft, P.R., Yan, J., and Zhang, J.H. (2013). Nasal administration of recombinant osteopontin attenuates early brain injury after subarachnoid hemorrhage. Stroke 44, 3189–3194.

31. Lindsey, M. L., Zouein, F.A., Tian, Y., PadmanabhanIyer, R., and de Castro Bras, L.E. (2015). Osteopontin is proteolytically processed by matrix metalloproteinase 9. Can. J. Physiol. Pharmacol. 93, 879–886.

32. Takafuji, V., Forgues, M., Unsworth, E., Goldsmith, P., and Wang, X.W. (2007). An osteopontin fragment is essential for tumor cell invasion in hepatocellular carcinoma. Oncogene, 26, 6361–6371.

33. Tan, T.K., Zheng, G., Hsu, T.T., Lee, S.R., Zhang, J., Zhao, Y., Tian, X., Wang, Y., Wang, Y.M., Cao, Q., Wang, Y., Lee, V.W., Wang, C., Zheng, D., Alexander, S.I., Thompson, E., and Harris, D.C. (2013). Matrix metalloproteinase-9 of tubular and macrophage origin contributes to the pathogenesis of renal fibrosis via macrophage recruitment through osteopontin cleavage. Lab. Invest. 93, 434–449.

34. Scatena, M., Liaw, L., and Giachelli, C.M. (2007). Osteopontin: a multifunctional molecule regulating chronic inflammation and vascular disease. Arterioscler. Thromb. Vasc. Biol. 27, 2302–2309.

35. Sun, S.-J., Wu, C.-C., Wu, G.-T., Sheu, G.-T., Chang, H.-Y., Chen, M.-Y., Lin, Y.-Y., Chuang, C.-Y., Hsu, S.-L., and Chang, J.T. (2015). Integrin b3 and CD44 levels determine the effects of the OPN—a splicing variant on lung cancer cell growth. Oncotarget 7, 55572–55584.

36. Ailane, S., Long, P., Jenner, P., and Rose, S. (2013). Expression of integrin and CD44 receptors recognizing osteopontin in the normal and LPS-lesioned rat substantia nigra. Eur. J. Neurosci. 38, 2468–2476.

37. Shin, T., Ahn, M., Kim, H., Moon, C., Kang, T.Y., Lee, J. M., Sim, K.B., and Hyun, J.W. (2005). Temporal expression of osteopontin and CD44 in rat brains with experimental cryolesions. Brain Res. 1041, 95–101.

38. Kang, W.S., Choi, J.S., Shin, Y.J., Kim, H.Y., Cha, J.H., Lee, J.Y., Chun, M.H., and Lee, M.Y. (2008). Differential regulation of osteopontin receptors, CD44 and the alpha(v) and beta(3) integrin subunits, in the rat hippocampus following transient forebrain ischemia. Brain Res. 1228, 208–216.

39. Gunther, M., Plantman, S., Davidsson, J., Angeria, M., Mathiesen, T., and Risling, M. (2015). COX-2 regulation and TUNEL-positive cell death differ between genders in the secondary inflammatory response following experimental penetrating focal brain injury in rats. Acta Neurochirurgica 157, 649–659.

40. Falo, M.C., Fillmore, H.L., Reeves, T.M., and Phillips, L.L. (2006). Matrix metalloproteinase-3 expression profile differentiates adaptive and maladaptive synaptic plasticity induced by traumatic brain injury. J. Neurosci Res. 84, 768–781.

41. Hadass, O., Tomlinson, B.N., Gooyit, M., Chen, S., Purdy, J.J., Walker, J.M., Zhang, C., Giritharan, A.B., Purnell, W., Robinson, C.R. II, Shin, D., Schroeder, V.A., Suckow, M.A., Simonyi, A., Sun, G.Y., Mobashery, S., Cui, J., Chang, M., and Gu, Z. (2013). Selective inhibition of matrix metalloproteinase-9 attenuates secondary damage resulting from severe traumatic brain injury. PLoS One, 8, e76904.

42. Reeves, T.M., Prins, M.L., Zhu, J., Povlishock, J.T., and Phillips, L.L. (2003). Matrix metalloproteinase inhibition alters functional and structural correlates of deafferentation-induced sprouting in the dentate gyrus. J. Neurosci. 23, 10182–10189.

43. Zhang, H., Trivedi, A., Lee, J.U., Lohela, M., Lee, S. M., Fandel, T.M., Werb, Z., and Noble-Haeusslein, L.J. (2011). Matrix metalloproteinase-9 and stromal cell-derived factor-1 act synergistically to support migration of blood-borne monocytes into the injured spinal cord. J. Neurosci. 31, 15894–15903.

44. Copin, J.C., Goodyear, M.C., Gidday, J.M., Shah, A.R., Gascon, E., Dayer, A., Morel, D.M., and Gasche, Y. (2005). Role of matrix metalloproteinases in apoptosis after transient focal cerebral ischemia in rats and mice. Eur. J. Neurosci. 22, 1597–1608.

45. Kaliszewska, A., Bijata, M., Kaczmarek, L., and Kossut, M. (2012). Experience-dependent plasticity of the barrel cortex in mice observed with 2-DG brain mapping and c-fos: effects of MMP-9 KO. Cereb. Cortex 22, 2160–2170.

46. Lee, S.R., Tsuji, K., Lee, S.R., and Lo, E.H. (2004). Role of matrix metalloproteinases in delayed neuronal damage after transient global cerebral ischemia. J. Neurosci. 24, 671–678.

47. Mizoguchi, H., Nakade, J., Tachibana, M., Ibi, D., Someya, E., Koike, H., Kamei, H., Nabeshima, T., Itohara, S., Takuma, K., Sawada, M., Sato, J., and Yamada, K. (2011). Matrix metalloproteinase-9 contributes to kindled seizure development in pentylenetetrazole-treated mice by converting pro-BDNF to mature BDNF in the hippocampus. J. Neurosci. 31, 12963–12971.

48. Wilczynski, G.M., Konopacki, F.A., Wilczek, E., Lasiecka, Z., Gorlewicz, A., Michaluk, P., Wawrzyniak, M., Malinowska, M., Okulski, P., Kolodziej, L.R., Konopka, W., Duniec, K., Mioduszewska, B., Nikolaev, E., Walczak, A., Owczarek, D., Gorecki, D.C., Zuschratter, W., Ottersen, O.P., and Kaczmarek, L. (2008). Important role of matrix metalloproteinase 9 in epileptogenesis. J. Cell Biol. 180, 1021–1035.

49. Van Hove, I., Lemmens, K., Van de Velde, S., Verslegers, M., and Moons, L. (2012). Matrix metalloproteinase-3 in the central nervous system: a look on the bright side. J. Neurochem. 123, 203–216.

50. Vu, T.H., Shipley, J.M., Bergers, G., Berger, J.E., Helms, J.A., Hanahan, D., Shapiro, S.D., Senior, R.M., and Werb, Z. (1998). MMP-9/gelatinase B is a key regulator of growth plate angiogenesis and apoptosis of hypertrophic chondrocytes. Cell, 93, 411–422.

51. Nagy, V., Bozdagi, O., Matynia, A., Balcerzyk, M., Okulski, P., Dzwonek, J., Costa, R.M., Silva, A.J., Kaczmarek, L., and Huntley, G.W. (2006). Matrix metalloproteinase-9 is required for hippocampal late-phase long-term potentiation and memory. J. Neurosci. 26, 1923–1934.

52. Graziadei, P.P., Levine, R.R., and Graziadei, G.A. (1978). Regeneration of olfactory axons and synapse formation in the forebrain after bulbectomy in neonatal mice. Proc. Natl. Acad. Sci. U. S. A. 75, 5230–5234.

53. Graziadei, P.P., Levine, R.R., and Monti Graziadei, G.A. (1979). Plasticity of connections of the olfactory sensory neuron: regeneration into the forebrain following bulbectomy in the neonatal mouse. Neuroscience 4, 713–727.

54. Morrison, E.E., and Costanzo, R.M. (1995). Regeneration of olfactory sensory neurons and reconnection in the aging hamster central nervous system. Neurosci. Lett. 198, 213–217.

55. Dixon, C.E., Lyeth, B.G., Povlishock, J.T., Findling, R.L., Hamm, R.J., Marmarou, A., Young, H.F., and Hayes, R.L. (1987). A fluid percussion model of experimental brain injury in the rat. J. Neurosurg. 67, 110–119.

56. Reeves, T.M., Smith, T.L., Williamson, J.C., and Phillips L.L. (2012). Unmyelinated axons show selective rostrocaudal pathology in the corpus callosum after traumatic brain injury. J. Neuropathol. Exp. Neurol. 71, 198–210.

57. Harris, L.K., Black, R.T., Reeves, T.M., and Phillips, L.L. (2012). Application of zymographic methods to study matrix enzymes following traumatic brain injury, in: *Animal Models of Acute Neurological Injuries II (vol.1): Injury and Mechanistic Assessments.* J. Chen, Z. Xu, X-M. Xu and J. Zheng (eds). Humana: New York, pps. 187–201.

58. Hill, J.W., Poddar, R., Thompson, J.F., Rosenberg, G.A., and Yang, Y. (2012). Intranuclear matrix metalloproteinases promote DNA damage and apoptosis induced by oxygen-glucose deprivation in neurons. Neuroscience 220, 277–290.

59. Woodcock, T., and Morganti-Kossmann, M.C. (2013). The role of markers of inflammation in traumatic brain injury. Front. Neurol. 4, 18.

60. Shin, S.-L., Cha, J.-H., Chun, M.-H., Chung, J.-W., and Lee, M.-Y. (1999). Expression of osteopontin mRNA in the adult brain. Neurosci. Lett. 273, 73–76.

61. Long, P., Samnakay, P., Jenner, P., and Rose, S. (2012). A yeast two-hybrid screen reveals that osteopontin associates with MAP1A and MAP1B in addition to other proteins linked to microtubule stability, apoptosis and protein degradation in the human brain. Eur. J. Neurosci. 36, 2733–2742.

62. Bakos, S.R., and Costanzo, R.J. (2011). Matrix metalloproteinase-9 is associated with acute inflammation after olfactory injury. Neuroreport 22, 539–543.

63. Abdul-Muneer, P.M., Pfister, B.J., Haorah, J., and Chandra, N. (2015). Role of matrix metalloproteinases in the pathogenesis of traumatic brain injury. Mol. Neurobiol. 53, 6106–6123.

64. Huntley, G.W. (2012). Synaptic circuit remodeling by matrix metalloproteinases in health and disease. Nature Rev. Neurosci. 13, 743–757.

65. Pastrana, E., Moreno-Flores, M.T., Gurzov, E.N., Avila, J., Wandosell, F., and Diaz-Nido, J. (2006). Genes associated with adult axon regeneration promoted by olfactory ensheathing cells: a new role for matrix metalloproteinase 2. J. Neurosci. 26, 5347–5359.

66. Li, Q., Michaud, M., Shankar, R., Canosa, S., Schwartz, M., and Madri, J.A. (2017). MMP-2: a modulator of neuronal precursor activity and cognitive motor behaviors. Behav. Brain Res. 333, 74–82.

67. Rosenberg, G.A. (1995). Matrix metalloproteinases in brain injury. J. Neurotrauma 12, 833–842.

68. Zhang, H., Adwanikar, H., Werb, Z., and Noble-Haeusslein, L.J. (2010). Matrix metalloproteinases and neurotrauma: evolving roles in injury and reparative processes. Neuroscientist 16, 156–170.

69. Agnihotri, R., Crawford, H.C., Haro, H., Matrisian, L.M., Havrda, M.C., and Liaw, L. (2001). Osteopontin, a novel substrate for matrix metalloproteinase-3 (stromelysin-1) and matrix metalloproteinase-7 (matrilysin). J. Biol. Chem. 276, 28261–28267.

70. Wang, K.X., and Denhardt, D.T. (2008). Osteopontin: role in immune regulation and stress responses. Cytokine Growth Factor Rev. 19, 333–345.

71. Weber, G.F., Ashkar, S., Glimcher, M.J., and Cantor, H. (1996). Receptor-ligand interaction between CD44 and osteopontin (Eta-1). Science 271, 509–512.

72. Shin, T. (2012). Osteopontin as a two-sided mediator in acute neuroinflammation in rat models. Acta Histochemica 114, 749–754.

73. Baliga, S.S., Merrill, G.F., Shinohara, M.L. and Denhardt, D.T. (2011). Osteopontin expression during early cerebral ischemia-reperfusion in rats: enhanced expression in the right cortex is suppressed by acetaminophen. PLoS One 6, e14568.

74. Sato, W., Tomita, A., Ichikawa, D., Lin, Y., Kishida, H., Miyake, S., Ogawa, M., Okamoto, T., Murata, M., Kuroiwa, Y., Aranami, T., and Yamamura, T. (2012).CCR2(+)CCR5(+) T cells produce matrix metalloproteinase-9 and osteopontin in the pathogenesis of multiple sclerosis. J. Immunol. 189, 5057–5065.

75. Choi, J.S., Kim, H.Y., Cha, J.H., Choi, J.Y. and Lee, M.Y. (2007). Transient microglial and prolonged astroglial upregulation of osteopontin following transient forebrain ischemia in rats. Brain Res. 1151, 195–202.

76. Ellison, J.A., Velier, J.J., Spera, P., Jonak, Z.L., Wang, X., Barone, F.C., and Feuerstein, G.Z. (1998). Osteopontin and its integrin receptor alpha(v)beta3 are upregulated during formation of the glial scar after focal stroke. Stroke 29, 1698–706.

77. vonGertten, C., Flores Morales, A., Holmin, S., Mathiesen, T., and Nordqvist, A.C. (2005). Genomic responses in rat cerebral cortex after traumatic brain injury. BMC Neurosci. 6, 69.

78. Kim, S.Y., Choi, Y.S., Choi, J.S., Cha, J.H., Kim, O.N., Lee, S.B., Chung, J.W., Chun, M.H., and Lee, M.Y. (2002). Osteopontin in kainic acid-induced microglial reactions in the rat brain. Mol. Cells 13, 429–435.

79. Plantman, S. (2012). Osteopontin is upregulated after mechanical brain injury and stimulates neurite growth from hippocampal neurons through beta1 integrin and CD44. Neuroreport 23, 647–652.

80. Bourguignon, L.Y., Gilad, E., Peyrollier, K., Brightman, A., and Swanson, R.A. (2007). Hyaluronan-CD44 interaction stimulates Rac1 signaling and PKN gamma kinase activation leading to cytoskeleton function and cell migration in astrocytes. J. Neurochem. 101, 1002–1017.

81. Desai, B., Ma, T., Zhu, J., and Chellaiah, M.A. (2009). Characterization of the expression of variant and standard CD44 in prostate cancer cells: identification of the possible molecular mechanism of CD44/MMP9 complex formation on the cell surface. J. Cell. Biochem. 108, 272–284.

82. Jones, L.L., Liu, Z., Shen, J., Werner, A., Kreutzberg, G.W., and Raivich, G. (2000). Regulation of the cell adhesion molecule CD44 after nerve transection and direct trauma to the mouse brain. J. Comp. Neurol. 426, 468–492.

83. Smith, L.L., Cheung, H.K., Ling, L.E., Chen, J., Sheppard, D., Pytela, R., and Giachelli, C.M. (1996). Osteopontin N-terminal domain contains a cryptic adhesive sequence recognized by alpha9beta1 integrin. J. Biol. Chem. 271, 28485–28491.

84. Gao, Y.A., Agnihotri, R., Vary, C.P., and Liaw, L. (2004). Expression and characterization of recombinant osteopontin peptides representing matrix metalloproteinase proteolytic fragments. Matrix Biol. 23, 457–466.

85. Maeda, K., Takahashi, K., Takahashi, F., Tamura, N., Maeda, M., Kon, S., Uede, T., and Fukuchi, Y. (2001). Distinct roles of osteopontin fragments in the development of the pulmonary involvement in sarcoidosis. Lung 179, 279–291.

86. Okamoto, I., Kawano, Y., Murakami, D., Sasayama, T., Araki, N., Miki, T., Wong, A.J., and Saya, H. (2001). Proteolytic release of CD44 intracellular domain and its role in the CD44 signaling pathway. J. Cell Biol. 155, 755–762.

87. Campo, G.M., Avenoso, A., D'Ascola, A., Scuruchi, M., Prestipino, V., Calatroni, A., and Campo, S. (2012). Hyaluronan in part mediates IL-1beta-induced inflammation in mouse chondrocytes by up-regulating CD44 receptors. Gene 494, 24–35.

88. Webb, D.S., Shimizu, Y., Van Seventer, G.A., Shaw, S., and Gerrard, T.L. (1990). LFA-3, CD44, and CD45: physiologic triggers of human monocyte TNF and IL-1 release. Science 249, 1295–1297.

89. Kobayashi, M., Tamari, K., Kitano, M., and Takeuchi, K. (2018). A time limit for initiating anti-inflammatory treatment for improved olfactory function after head injury. J. Neurotrauma 35, 652–660.

90. Monti-Graziadei, G.A., Margolis, F.L., Harding, J.W. and Graziadei, P.P. (1977). Immunocytochemistry of the olfactory marker protein. J. Histochem. Cytochem. 25, 1311–1316.

91. Harding, J., Graziadei, P.P., Monti-Graziadei, G.A., and Margolis, F.L. (1977). Denervation in the primary olfactory pathway of mice. IV. Biochemical and morphological evidence for neuronal replacement following nerve section. Brain Res. 132, 11–18.

92. Cummings, D.M., Emge, D.K., Small, S.L., and Margolis, F.L. (2000). Pattern of olfactory bulb innervation returns after recovery from reversible peripheral deafferentation. J. Comp. Neurol. 421, 362–373.

93. Holbrook, E.H., Iwema, C.L., Peluso, C.E., and Schwob, J.E. (2014). The regeneration of P2 olfactory sensory neurons is selectively impaired following methyl bromide lesion. Chem. Senses 39, 601–616.

94. Kasowski, H.J., Kim, H., and Greer, C.A. (1999). Compartmental organization of the olfactory bulb glomerulus. J. Comp. Neuro. 407, 261–274.

95. Kosaka, K., Aika, Y., Toida, K., and Kosaka, T. (2001). Structure of intraglomerular dendritic tufts of mitral cells and their contacts with olfactory nerve terminals and calbindin-immunoreactive type 2 periglomerular neurons. J. Comp. Neurol. 440, 219–235.

96. Ethell, I.M., and Ethell, D.W. (2007). Matrix metalloproteinases in brain development and remodeling: Synaptic functions and targets. J. Neurosc. Res. 85, 2813–2823.

97. Monea, S., Jordan, B.A., Srivastava, S., DeSouza, S., and Ziff, E.B. (2006). Membrane localization of membrane type 5 matrix metalloproteinase by AMPA receptor binding protein and cleavage of cadherins. J. Neurosci. 26, 2300–2312.

98. Muradashvili, N., Tyagi, N., Tyagi, R., Munjal, C., and Lominadze, D. (2011). Fibrinogen alters mouse brain endothelial cell layer integrity affecting vascular endothelial cadherin. Biochem. Biophys. Res. Comm. 413, 509–514.

99. Lu, D.Y., Yeh, W.L., Huang, S.M., Tang, C.H., Lin, H.Y., and Chou, S.J. (2012). Osteopontin increases heme oxygenase-1 expression and subsequently induces cell migration and invasion in glioma cells. Neuro-Oncol. 14, 1367–1378.

100. Ding, Q., Stewart, J.,Jr, Prince, C. W., Chang, P. L., Trikha, M., Han, X., Grammer, J.R., and Gladson, C.L. (2002). Promotion of malignant astrocytoma cell migration by osteopontin expressed in the normal brain: differences in integrin signaling during cell adhesion to osteopontin versus vitronectin. Cancer Res. 62, 5336–5343.

101. Shubayev, V.I., and Myers, R.R. (2004). Matrix metalloproteinase-9 promotes nerve growth factor-induced neurite elongation but not new sprout formation in vitro. J. Neurosci. Res. 77, 229–239.

102. Kelly, E.A., Russo, A.S., Jackson, C.D., Lamantia, C.E., and Majewska, A.K. (2015). Proteolytic regulation of synaptic plasticity in the mouse primary visual cortex: analysis of matrix metalloproteinase 9 deficient mice. Front. Cell. Neurosci. 9, 369.

Address correspondence to:
Linda L. Phillips, PhD
Department of Anatomy and Neurobiology
Medical Campus, Virginia Commonwealth University
PO Box 980709
Richmond, VA 23298

E-mail: Linda.Phillips@vcuhealth.org